Update a biogeochemical model with process-based algorithms to predict ammonia volatilization from fertilized **cultivated** uplands and rice paddy fields

Siqi Li[1], Wei Zhang[1], Xunhua Zheng[1,2], Yong Li[1], Shenghui Han[1], Rui Wang[1], Kai Wang[1], Zhisheng Yao[1], Chunyan Liu[1], Chong Zhang[3]

[1]State Key Laboratory of Atmospheric Boundary Layer Physics and Atmospheric Chemistry, Institute of Atmospheric Physics, Chinese Academy of Sciences, Beijing 100029, P. R. China

[2]College of Earth and Planetary Science, University of Chinese Academy of Sciences, Beijing 100049, P.R. China

[3]College of Tropical Crops, Hainan University, Haikou 570228, China

Correspondence to: Xunhua Zheng (xunhua.zheng@post.iap.ac.cn)

Yong Li (yli@mail.iap.ac.cn)

Abstract. Accurate simulation of ammonia (NH_3) volatilization from fertilized croplands is crucial to enhancing fertilizer-use efficiency and alleviating environmental pollution. In this study, a process-oriented model, CNMM-DNDC (Catchment Nutrient Management Model - DeNitrification-DeComposition), was evaluated and modified using NH_3 volatilization observations from 44 and 19 fertilizer application events in cultivated uplands~~ areas~~ and paddy rice fields in China, respectively. ~~The original CNMM-DNDC model not only performed poorly in simulating NH₃ volatilization from upland areas but also failed to simulate NH₃ volatilization from paddy rice fields.~~ ~~In the modified CNMM-DNDC model, t~~The major modifications for simulating NH_3 volatilization from **cultivated** uplands were primarily derived from a peer-reviewed and published study. NH_3 volatilization from **cultivated** uplands was jointly regulated by ~~the factors of~~ wind speed, soil depth, clay fraction, soil temperature, soil moisture, vegetation canopy, and rainfall-induced canopy wetting. Moreover, three principle modifications were made to simulate NH_3 volatilization from paddy rice fields. First, the simulation of the floodwater layer and its pH were added. Second, the effect of algal growth on the diurnal fluctuation of floodwater pH was introduced. Finally, the Jayaweera-Mikkelsen model was introduced to simulate NH_3 volatilization. The results indicated that the original CNMM-DNDC ~~model~~ not only performed poorly in simulating NH_3 volatilization from **cultivated** uplands~~ areas~~ but also failed to simulate NH_3 volatilization from paddy rice fields. The modified model showed

remarkable performances in simulating the cumulative NH_3 volatilization of the calibrated and validated cases, with drastically significant zero-intercept linear regression of slopes of 0.94 ($R^2 = 0.76$, $n = 40$) and 0.98 ($R^2 = 0.71$, $n = 23$), respectively. The simulated NH_3 volatilization from cultivated uplands was primarily regulated by the dose and type of the nitrogen fertilizer and the irrigation implementation, while the simulated NH_3 volatilization from rice paddy fields was sensitive to soil pH, the dose and depth of nitrogen fertilizer application, and flooding management strategies, such as floodwater pH and depth. However, the volatilized NH_3 simulated by the modified model still exhibited some deviation from the observations when deep/mixed placement, irrigation/precipitation, and prosperous/depressed algal biomass accompanied the fertilizer application events. Future studies still need to solve these problems to further improve the performance of the modified model. Nevertheless, Tthe modified model is acceptable to compile regional or national could provide an available method for developing NH_3 emission inventories and reducing developing strategies to alleviate environmental pollutions.

1. Introduction

Synthetic fertilizer application, as the secondary largest contributor to ammonia (NH_3) emissions after livestock production, accounts for approximately 30% to 50% of anthropogenic NH_3 emissions (Behera et al., 2013; Bouwman et al., 1997; Huang et al., 2012; Paulot et al., 2014). The great quantity of NH_3 volatilized from agricultural fields contributes to low nitrogen use efficiency for crops (Chien et al., 2009; Mariano et al., 2019; Zhu et al., 1989). The subsequent dry and wet deposition to terrestrial ecosystems results in the acidification and eutrophication of natural ecosystems (e.g., Anderson et al., 2008; Bobbink et al., 1998; Li et al., 2016) and is also considered an indirect source of nitrous oxide (Martin et al., 2004; Schjørring, 1998). Recently, NH_3 in the atmosphere has played a vital role in aerosol formation during several haze periods, which has attracted great attention (e.g., Felix et al., 2013; Kong et al., 2019; Liu et al., 2018; Savard et al., 2017).

Many studies have attempted to estimate NH_3ammonia loss from fertilized croplands using biogeochemical process models, i.e., DeNitrification-DeComposition (DNDC), and water and nitrogen management (WNMM) and CESM (Dubache et al., 2019; Dutta et al., 2016; Giltrap et al., 2017;

Michalczyk et al., 2016; Park et al., 2008; Riddick et al., 2016; Vira et al., 2020). However, these models do not distinguish between the simulation modules of NH_3 volatilization for cultivated uplands and rice paddy fields but rather use the same algorithm (Cannavo et al., 2008; Li, 2016). It is worth emphasizing that the mechanisms of NH_3 volatilization are completely different between cultivatedfertilized uplands and rice paddy fields due to the presence of floodwater over rice paddy soils. Recent studies also indicate that estimating NH_3 emissions without considering rice cultivation results in large uncertainties (Riddick et al., 2016; Xu et al., 2019). In particular, some studies have shown that NH_3 volatilization rates from rice paddy fields are not lower than those of upland crops (Zhou et al., 2016), which also indicates the different mechanisms of NH_3 volatilization between cultivatedfertilized uplands and rice paddy fields. Therefore, using separate modules to simulate NH_3 volatilization from cultivated uplands and rice paddy fields is necessary for the accurate estimation of NH_3 emissions.

Given the totally different mechanisms of NH_3 volatilization between cultivatedfertilized uplands and rice paddy fields, the influencing factors affecting NH_3 volatilization from cultivated uplands are different from those of rice paddy fields. The dose, type and application methods of nitrogen fertilizer have been confirmed as the primary factors affecting NH_3 volatilization from cultivated uplands (e.g., Liu et al., 2003; Roelcke et al., 2002; Zhang et al., 1992). Moreover, several studies have reported that irrigation and precipitation exert a complicated influence (stimulated or inhibited) on NH_3 volatilizations from cultivated uplands soils (e.g., Han et al., 2014; Holcomb III et al., 2011; Sanz-Cobena et al., 2011). However, the depth and pH of surface floodwater, which are unique characteristics of rice paddy fields, were found to be the major factors influencing NH_3 volatilization from rice paddy fields (Bowmer and Muirhead, 1987; Hayashi et al., 2006; Jayaweera and Mikkelsen, 1991). A comprehensive discussion of the influencing factors affecting NH_3 volatilization from cultivated uplands and rice paddy fields is crucial for providing suggestions to further improve the performance of process-based biogeochemical models in simulating NH_3 volatilization from cropland soils and offer specific and pertinent policy advice for the reduction of NH_3ammonia loss.

A previous study established a scientific algorithm for the DNDC model to simulate NH_3 volatilization from cultivated fertilized uplands soils, which performed well under validation with

85 independent cases of cultivated uplands from China (Li et al., 2019). However, no biogeochemical

86 model has achieved simulations of NH_3 volatilization from rice paddy fields using a process-oriented

87 algorithm, although a classical and extensively used model, i.e., the Jayaweera-Mikkelsen model (J-M

88 model), exists (Jayaweera and Mikkelsen, 1990a; Li et al., 2008; Wang et al., 2016; Zhan et al., 2019).

89   The Catchment Nutrient Management Model-DeNitrification-DeComposition (CNMM-DNDC)

90 model, established by coupling the core carbon and nitrogen biogeochemical processes of DNDC (e.g.,

91 decomposition, nitrification, denitrification and fermentation) into the distributed hydrologic

92 framework of CNMM, is one of the latest versions of DNDC (Zhang et al., 2018). The CNMM-DNDC

93 has been gradually developing into a comprehensive and reliable process-oriented biogeochemical

94 model that performs well in terms of simulating the complex hydrologic and biogeochemical processes

95 of a subtropical catchment with various landscapes (Zhang et al., 2018), the nitrous oxide and nitric

96 oxide emissions from a subtropical tea plantation (Zhang et al., 2020) and the NO_3^- leaching processes

97 of black soils in northeastern China (Zhang et al., 2021). However, the rationality of the

98 CNMM-DNDC's scientific processes in simulating NH_3 volatilization from fertilized croplands is still

99 lacking in terms of a thorough assessment. In particular, CNMM-DNDC and other widely used

100 biogeochemical models (e.g., DNDC) do not consider floodwater over rice paddy soils when

101 simulating NH_3 volatilization but rather directly adopt the scientific processes and algorithms applied

102 in NH_3 volatilization from cultivated uplands to predict NH_3 volatilization from rice paddy fields (Li,

103 2016; Zhang et al., 2018).

104   Based on the above deficiencies, the authors hypothesized that the CNMM-DNDC is able to

105 simulate NH_3 volatilization following the application of synthetic nitrogen fertilizers to cultivated

106 uplands and flooded rice paddy fields. To test this hypothesis, this study evaluated and modified the

107 CNMM-DNDC's scientific processes for simulating NH_3 volatilization from cropland soils using 44

108 and 19 fertilizer application events from cultivated uplands and rice paddy fields in China, respectively.

109 The objectives of this study were to (i) evaluate the performance of the CNMM-DNDC in simulating the

110 observed NH_3 volatilization following synthetic nitrogen application to cultivated uplands, (ii) introduce

111 thoroughly tested and validated scientific algorithms simulating NH_3 volatilization from cultivated

112 uplands into the CNMM-DNDC, (iii) adopt widely applied process-based algorithms (J-M model) into

the modified CNMM-DNDC, (iv) assess the performance of the modified model to simulate NH_3 volatilization from flooded rice paddy fields using collected reliable observations, and (v) identify the major factors affecting NH_3 volatilization from cultivated uplands and rice paddy fields to offer suggestions for further improving the model performance.

2. Materials and methods

~~2.1 Brief description of the field sites and treatments~~

~~Two field observation datasets of NH_3 volatilization using micrometeorological methods or wind tunnel techniques, which were measured in cultivated uplands and flooded rice paddy fields of China, respectively, were collected from published peer reviewed articles. For the dataset of cultivated uplands, the collected field observations were conducted at seven experimental sites, including Dongbeiwang (DBW) in Beijing; Fengqiu with uplands (FQU) in Henan; Guangchuan (GC) Luancheng (LC), and Quzhou (QZ) in Hebei; Yanting (YT) in Sichuan; and Yongji (YJ) in Shanxi (Fig. 1), and the dataset were directly inherited from Li et al. (2019). The upland sites involved in this study were calcareous soils cultivated with summer maize and winter wheat. The 44 cases of synthetic fertilizer application events in the cultivated uplands involved various fertilizer types (including urea, ammonium bicarbonate (ABC), ammonium sulfate, and complex fertilizer), a wide range of applied fertilizer doses ($60-348$ kg N ha^{-1}), and various agricultural management practices (e.g., broadcast or deep point placement of fertilizer(s) alone or fertilization coupled with irrigation). For the rice paddy field dataset, field observations were collected at five experimental sites, including Changshu (CS) and Danyang (DY) in Jiangsu, Fengqiu with rice paddy fields (FQP) in Henan, Shenzhen (SZ) in Guangdong, and Yingtan (YTA) in Jiangxi (Fig. 1), and these sites were cultivated with summer rice and winter wheat or double rice (Table 1). In total, nineteen (P1-P19) synthetic fertilizer application events were included in these measurements, covering different fertilizer types, including urea and ABC; fertilizer doses in the range of $41-162$ kg N ha^{-1}; and various agricultural management practices (e.g., broadcasting or broadcasting followed by tillage, Table 1 and Table 2). In addition, the other auxiliary variables, e.g., temperature, pH, and ammonium (NH_4^+) concentration of the floodwater, measured in the rice paddy experimental sites during the NH_3 volatilization measurement periods were also~~

140 collected for model calibration and validation.

2.12 Model introduction and modifications

2.21.1 Brief introduction of the CNMM-DNDC

The CNMM-DNDC model used in this study was originallyfirst established by Zhang et al. (2018). by incorporating tIn the original CNMM-DNDC, the core biogeochemical processes (including decomposition, nitrification, denitrification and fermentation) of DNDC (Li, 2016; Li et al., 1992) were incorporated into the distributed hydrologic framework of CNMM (Li et al., 2017). Based on comprehensive observations, the CNMM-DNDC was initially tested in a subtropical catchment, which showed credible performances in simulating the yields of crops, emissions of greenhouse gases (i.e., methane and nitrous oxide), emissions of nitrogenous pollutant gases (i.e., nitric oxide and NH_3ammonia), and hydrological nitrogen losses by leaching and NO_3^- discharge in streams for different land uses (including forests and arable lands cultivated with maize, wheat, oil rape, or rice paddy) (Zhang et al., 2018). Subsequently, Zhang et al. (2020) modified the CNMM-DNDC by adding tea growth-related processes that may induce a soil pH reduction, and this modified model performed well in simulating the emissions of nitrous oxide and nitric oxide from a subtropical tea plantation plot. Moreover, the CNMM-DNDC performed well in simulating the NO_3^- leaching process of black soils in northeastern China (Zhang et al., 2021). However, during model preparation and operation for the simulation of NH_3 volatilization, the authors found that the present model version, using a complicated and obscure R programming script to prepare the ARC GRID ASCII data format of site/plot-scale inputs, was time-consuming and confusing. Therefore, an easy-to-operate and standardized version of the model needed to be established. Thus, a standardized model version was established in this study.

The new standard version of the model was built without changing the original key scientific modules; however, the complicated R programming script was converted into a simple Excel spreadsheet to prepare the model inputs, which is easy for beginners to use. The site-scale and regional-scale simulations were separated. In the site-scale simulation used in this study, the authors hypothesized a flat terrain region with a 5×5 grid, and thus, the solar radiation was not affected by topography. Therefore, the simulation of any grid was the same and could be regarded as the

167 representative simulation results of the study region. If the users were only interested in the simulation

168 of a field site experiment or could only provide the input data based on the site/plot scale, then they

169 would not need to provide any information about the topography and stream of their study region

170 which were necessary prepared in the regional-scale simulation. The~~is~~ site-scale simulation, which was

171 used in this study, is convenient for model validation, saves time in terms of model operation, and is

172 easy to use for beginners.

173 **2.~~2~~1.2 Modifications for simulating NH$_3$~~ammonia~~ volatilization from cultivated uplands**

174 In the original CNMM-DNDC model, the direct processes involved in the calculation of NH$_3$

175 volatilization from cultivated uplands included ammonium bicarbonate (ABC) decomposition, urea

176 hydrolysis and NH$_3$ volatilization (Fig. S1). Among them, ABC decomposition was regulated by soil

177 pH and soil depth; urea hydrolysis was affected by soil temperature and soil organic carbon; NH$_3$

178 volatilization from cultivated uplands was simply determined by the regulating factors of wind speed,

179 soil depth and soil temperature (Table S1 and S2). Moreover, other synthetic fertilizers dissolution and

180 organic manure mineralization were involved in the original model. The modifications of the new

181 version of the CNMM-DNDC for simulating NH$_3$ volatilization from cultivated uplands were mainly

182 adapted from Li et al. (2019). Compared to the original CNMM-DNDC, ~~the authors conducted~~ three

183 major modifications were conducted ~~in terms of the new version~~. First, the soil temperature parameter

184 (f_T)~~s~~ of the urea hydrolysis function was~~were~~ recalibrated and the effect of soil moisture on urea

185 hydrolysis (f_{SM}) was newly added. Second, the regulatory effect of soil temperature on ABC

186 decomposition (f_{Ts_ABC}) was parameterized. Finally, the effects of the original parameters of ~~wind,~~ soil

187 temperature and moisture on NH$_3$ volatilization were recalibrated, and the effects of the clay fraction,

188 plant standing, and canopy wetting on NH$_3$ release to the atmosphere were newly parameterized (Fig.

189 S1). The above-mentioned calibration and parameterization were conducted by Dubache et al. (2019)

190 and Li et al. (2019). Therefore, the NH$_3$~~ammonia~~ flux from cultivated uplands (flux (NH$_3$)$_{uplands}$) was

191 jointly determined by the regulating factors of wind speed (f_{wind}, 0−1), soil temperature (f_{temp}, 0−1), soil

192 moisture (f_{water}, 0−1), soil depth (f_{depth}, 0−1), clay fraction (f_{clay}, 0−1), vegetation canopy (f_{canopy}, 0−1),

193 and rainfall-induced canopy wetting (f_{rain}, 0−1), as shown in Eq. (1). Each factor was defined as a

194 dimensionless fraction within 0–1. $NH_{3(l)}$ is referred to as the dissolved NH_3 in the liquid phase of

195 upland soils. Among these regulating factors, f_{depth} was calculated by the number of soil layers in Li et

196 al. (2019), where the thickness of the soil layer was set as the value of the saturated hydraulic

197 conductivity. However, in the CNMM-DNDC, the simulated soil layers and their corresponding

198 thicknesses were set to be freely defined by users. The algorithm of f_{depth} from Li et al. (2019) was

199 inappropriate for this study. Therefore, f_{depth} was revised using the thickness of the soil layer based on

200 Eq. (2), wherein d_{soil} denotes the depth of the simulated soil layer. The calibration cases with fertilizer

201 application depth were used for the calibration of f_{depth}. Moreover, the time step of the CNMM-DNDC

202 was three hours, but the time step was one day in the DNDC model. So the ratio of time steps of the

203 two models (T_{layer} with the value of 8) was involved in Eq. (1). Nevertheless, ~~To solve~~ the ~~simulation~~

204 deviation between derived from the different time steps ~~existed~~, as shown in Table S3. To solve the

205 deviation~~derived from the different time steps~~, a time-step parameter (f_{Tstep}, ~~0–1~~) was introduced into

206 Eq. (1), which was calculated at 0.75 in this study using the calibration cases with surface broadcast (n

207 $= 21$). The zero-intercept linear regression was applied for model calibration. We provided the

208 calibration of f_{Tstep} in Fig. S2 as an instance. Table S1 listed the algorithms of the original and modified

209 model in simulating NH_3 volatilization from cultivated uplands. The descriptions and units of the

210 symbols used in Table S1 were listed in Table S2.

$$Flux(NH_3)_{upland} = 3.6 f_{wind} f_{temp} f_{water} f_{depth} f_{clay} f_{canopy} f_{rain} f_{Tstep} NH_{3(l)} / T_{layer} \qquad (1)$$

$$f_{depth} = 0.5^{d_{soil}/0.03} \qquad (2)$$

211

212 **2.~~2~~1.3 Modifications for simulating NH_3~~ammonia~~ volatilization from rice paddy fields**

213   The original CNMM-DNDC failed to simulate NH_3 volatilizations from rice paddy fields because

214 it lacked the capability to simulate the surface water-flooded layer over rice paddy fields. Given the

215 presence of floodwater over rice paddy soils, the mechanisms of NH_3 volatilization are different

216 between cultivated uplands and rice paddy fields. However, CNMM-DNDC and other widely used

217 biogeochemical models (e.g., DNDC) adopted scientific processes and algorithms applied in simulating

218 NH_3 volatilization from fertilized cultivated uplands to calculate NH_3 volatilization from rice paddy

219   fields without considering floodwater over soils (Cannavo et al., 2008; Li, 2016). Therefore, floodwater

220   over rice paddy soils was added to the modified CNMM-DNDC. To add this component, the modified

221   CNMM-DNDC adopted the Jayaweera-Mikkelsen model (i.e., J-M model), based on the two-film

222   theory of mass transfer (Jayaweera and Mikkelsen, 1990a), which is one of the most widely applied

223   process-based models for simulating NH_3 volatilization from rice paddy fields. The J-M model consists

224   of two processes (Fig. 2): (i) the chemical processes of NH_4^+ ions and aqueous NH_3 ($NH_{3(aq)}$)

225   equilibrium in floodwater and (ii) the volatilization processes of $NH_{3(aq)}$ transfer in the form of NH_3 gas

226   ($NH_{3(air)}$) across the water-air interface to the atmosphere (Rxn1). k_d (first-order, s^{-1}) and k_a

227   (second-order, $L\ mol^{-1}\ s^{-1}$) are referred to as the dissociation and association rate constants for

228    $NH_4^+/NH_{3(aq)}$ equilibrium, respectively. k_{vN} (first-order, s^{-1}) is referred to as the volatilization rate

229   constant of $NH_{3(aq)}$.

$$NH_4^+ \underset{k_a}{\overset{k_d}{\rightleftharpoons}} H^+ + NH_{3(aq)} \xrightarrow{k_{vN}} NH_{3(air)} \tag{Rxn1}$$

230   According to the above theories, the change rate of the NH_4^+ concentration in floodwater ($[NH_4^+]_w$,

231    $mol\ L^{-1}$) due to NH_3 volatilization (R_a, $mol\ L^{-1}\ s^{-1}$) can be estimated by Eq. (3) as a function of

232    $[NH_4^+]_w$, H^+ concentration in floodwater ($[H^+]_w$, $mol\ L^{-1}$), k_d, k_a and k_{vN}.

$$R_a = -\frac{k_d k_{vN} [NH_4^+]_w}{k_a [H^+]_w + k_{vN}} \tag{3}$$

233   The dynamic changes in $[H^+]_w$ and $[NH_4^+]_w$ are calculated by the CNMM-DNDC instead of the

234   field experiment described in Jayaweera and Mikkelsen (1990a).

235   In the modified CNMM-DNDC, the pH of the floodwater, which is the negative logarithm of

236    $[H^+]_w$, is related to the initial pH of water for flooding and that of surface soil. When the floodwater

237   depth is less than 0.04 m, the pH of the floodwater is equal to the mean of the initial pH of water for

238   flooding and that of surface soil, both of which are the inputs of the modified model. Otherwise, the pH

239   of the floodwater is equal to the initial pH of the water for flooding. On the one hand, $[H^+]_w$ is regulated

240   by urea hydrolysis in floodwater, the algorithm of which was derived from that of urea hydrolysis

241   affecting soil pH in the model. On the other hand, many studies have found that a marked diurnal

242   fluctuation in floodwater pH is associated with algal photosynthesis, which was elevated with solar

243   radiation (De Datta, 1995; Fillery and Vlek, 1986). Therefore, a ratio of the daytime solar shortwave

244 radiation effect on algal photosynthesis (R_{slr}, 0−1) was established by the authors using Eq. (4) as a

245 quadratic function of the simulation time (t, 06:00 to 21:00 with a 3-hour interval) of a day. R_{slr} at the

246 other moments with no or extremely little solar radiation in a day was set as 0. The effect of algal

247 growth (f_{alg}) on floodwater pH was calculated by Eq. (5), where the adjusted coefficient (k_{alg}, 0−1) was

248 calibrated to 0.75 or 0.6 when the floodwater depth was no more than or more than 0.04 m, respectively.

249 The floodwater pH of (t+1)th was modified by the floodwater pH of tth and f_{alg} using Eq. 6, which was

250 set as no more than 10.

$$R_{slr} = -0.0036t^2 + 0.1096t - 0.7046 \tag{4}$$

$$f_{alg} = k_{alg}R_{slr}R + 0.25 \tag{5}$$

$$pH_{t+1} = pH_t + f_{alg} \tag{6}$$

251   When fertilizers (e.g., urea) are applied to the rice paddy fields, they are first allocated to the

252 floodwater and soil layers according to the ratio of the floodwater depth and the application depth of

253 fertilizer in the modified CNMM-DNDC. Subsequently, $[NH_4^+]_w$ increases with urea hydrolysis, and

254 ABC decomposition occurs in the floodwater. In the modified model, the calculation of urea hydrolysis

255 in floodwater refers to that in the upland soils (Dubache et al., 2019) by removing the influencing

256 factors of soil organic carbon and soil moisture. Therefore, urea hydrolysis in floodwater is only

257 determined by the floodwater temperature. To simplify the calculation, the floodwater temperature is

258 arbitrarily set equal to the temperature in the first soil layer in the modified model. Given that ABC

259 decomposition in floodwater was not involved in the original CNMM-DNDC, this study directly

260 adopted the algorithm of ABC decomposition in upland soils used in Li et al. (2019), and this process

261 was regulated by soil temperature, pH and the applied depth of fertilizer. However, ABC decomposition

262 in floodwater is different from that in upland soils; i.e., the ABC concentration is uniformly distributed

263 in the floodwater, and the effect factors (i.e., temperature, pH and depth) applied should be those of

264 floodwater rather than those of soil. Therefore, this study ignored the effect of soil depth and retained

265 the effect of floodwater temperature and pH on ABC decomposition in floodwater.

266   For each simulation time step, the NH_4^+ in the floodwater and the first soil layer experiences

267 uniform mixing and exchange. Then, NH_4^+ is transported in soil layers, accompanied by organic

268 nitrogen mineralization, consumption via plant uptake, nitrification, volatilization of NH_3, and

269 adsorption/desorption by clay (Li, 2016; Li et al., 1992; Li et al., 2019).

270 k_d, k_a and k_{vN} in Eq. (3) are determined by the environmental factors, i.e., the temperature and the

271 depth of floodwater (Jayaweera and Mikkelsen, 1990a). As shown in Eq. (7), k_a is affected by its

272 relationship with floodwater temperature (T_f, K) based on Alberty (1983):

$$k_a = 3.8 \times 10^{11} - 3.4 \times 10^9 T_f + 7.5 \times 10^6 T_f^{\ 2} \tag{7}$$

273 k_d is derived from the relationship with the equilibrium constant for $NH_4^+/NH_{3(aq)}$ (K) and k_a (Eq.

274 (8)):

$$k_d = Kk_a \tag{8}$$

275 K is calculated as a function of the floodwater temperature (Eq. (9)) derived from Jayaweera and

276 Mikkelsen (1990a):

$$K = 10^{-[0.0897 + (2729/T_f)]} \tag{9}$$

277 The NH_3 volatilization rate constant (k_{vN}) is estimated by the law of conservation of mass, which

278 is considered in the system of NH_3 transfer across the air-water interface. By dimensional analysis, k_{vN}

279 is determined by Eq. (10), based on the ratio of the floodwater depth (d, m) and the overall

280 mass-transfer coefficient for NH_3 (K_{ON}, cm h^{-1}):

$$k_{vN} = K_{ON} / (3.6 \times 10^5 d) \tag{10}$$

281 According to the two-film theory, based on Fick's first law and Henry's law, K_{ON} is determined by

282 Eq. (11) using the exchange constant for NH_3 in the gas and liquid phases (k_{gN} and k_{lN}, respectively)

283 and the non-dimensional Henry's constant (H_{nN}). As described by Jayaweera and Mikkelsen (1990a),

284 H_{nN} is a function of T_f, which can be calculated by Eq. (12), whereas k_{gN} and k_{lN} are dependent on the

285 wind speed measured at a height of 8 m (U_8, m s^{-1}), which can be calculated using Eqs. (13−14). U_8

286 can be determined using the model input of wind speed measured at a height of 10 m (U_{10}, m s^{-1}),

287 based on Eq. (15) derived from Jayaweera and Mikkelsen (1990a).

$$K_{ON} = (H_{nN} k_{gN} k_{IN}) / (H_{nN} k_{gN} + k_{IN}) \tag{11}$$

$$H_{nN} = 183.8 e^{(-1229/T_f)} / R T_f \tag{12}$$

$$k_{gN} = 19.0895 + 742.3016 U_8 \tag{13}$$

$$k_{IN} = \left\{ 12.5853 / \left[1 + 43.0565 e^{(-0.4417 U_8)} \right] \right\} / 1.6075 \tag{14}$$

$$U_8 = \frac{11.51}{\ln(10/8 \times 10^5)} U_{10} \tag{15}$$

288   Finally, the three-hour cumulative flux of NH$_3$ volatilization (Flux (NH$_3$)$_{rice}$, kg N ha^{-1} 3h^{-1}) is

289   calculated by Eq. (16) using R_a, d, and the simulation time step based on the molar mass of N (~14 g

290   mol^{-1}) and the conversion coefficient from m^2 to ha (1 m^2 = 1 × 10^{-4} ha).

$$\text{Flux}(\text{NH}_3)_{rice} = -1.512 \times 10^9 d R_a \tag{16}$$

291   The CNMM-DNDC with the above modifications is hereinafter referred to as the modified

292   CNMM-DNDC. ~~The cases for model calibration were identified on the basis of covering as many~~

293   ~~climate conditions, soil properties and management practices as possible. Therefore, for the simulation~~

294   ~~of NH$_3$ from urea application on uplands and rice paddy fields, 26 typical cases of DBW, FQU, and QZ~~

295   ~~and 10 typical cases of DY, FQP, and SZ were used for model calibration. Regarding the simulation of~~

296   ~~NH$_3$ from the ABC application on uplands and rice paddy fields, 3 typical cases of DBW and YT and 1~~

297   ~~typical DY case were conducted for model calibration. The remaining 23 independent cases were~~

298   ~~provided for model validation.~~

299   **2.2 Brief description of the field sites and treatments**

300   Two field observation datasets of NH$_3$ volatilization using micrometeorological methods or wind

301   tunnel techniques, which were measured in cultivated uplands and flooded rice paddy fields of China,

302   respectively, were collected from published peer-reviewed articles. For the dataset of cultivated uplands,

303   the collected field observations were conducted at seven experimental sites, including Dongbeiwang

304   (DBW) in Beijing; Fengqiu with cultivated uplands (FQU) in Henan; Guangchuan (GC) Luancheng

305   (LC), and Quzhou (QZ) in Hebei; Yanting (YT) in Sichuan; and Yongji (YJ) in Shanxi (Fig. 1), and the

306   dataset were directly inherited from Li et al. (2019). The upland sites involved in this study were

calcareous soils cultivated with summer maize and winter wheat. The 44 cases of synthetic fertilizer application events in cultivated uplands (Table S4) involved various fertilizer types (including urea, ammonium bicarbonate (ABC), ammonium sulfate, and complex fertilizer), a wide range of applied fertilizer doses (60–348 kg N ha^{-1}), and various agricultural management practices (e.g., broadcast or deep point placement of fertilizer(s) alone or fertilization coupled with irrigation). For the rice paddy field dataset, field observations were collected at five experimental sites, including Changshu (CS) and Danyang (DY) in Jiangsu, Fengqiu with rice paddy fields (FQP) in Henan, Shenzhen (SZ) in Guangdong, and Yingtan (YTA) in Jiangxi (Fig. 1), and these sites were cultivated with summer rice and winter wheat or double rice (Table 1). In total, nineteen (P1–P19) synthetic fertilizer application events were included in these measurements, covering different fertilizer types, including urea and ABC; fertilizer doses in the range of 41–162 kg N ha^{-1}; and various agricultural management practices (e.g., broadcasting or broadcasting followed by tillage, Table 1 and Table 2). In addition, the other auxiliary variables, e.g., temperature, pH, and ammonium (NH_4^+) concentration of the floodwater, measured in the rice paddy experimental sites during the NH_3 volatilization measurement periods were also collected for model calibration and validation.

2.3 Model preparation and operation

2.3.1 Input data formatting

The input data of the modified CNMM-DNDC used in this study included the meteorological conditions of the study area (e.g., 3-hourly average air temperature (T_{air}), precipitation (P), wind speed (W), solar radiation (R), relative humidity (RH)), the necessary soil properties of individual layers (e.g., soil clay and sand fraction, organic carbon (SOC), bulk density (BD), pH), crop parameters (e.g., crop type, thermal degree days for maturity (TDD), nitrogen content, plant height and root depth), and the implemented management practices (e.g., plant and harvest dates, methods and/or amounts of individual management practices including fertilization, tillage, irrigation and flooding).

For the meteorological data inputs, the reported 3-hourly meteorological data from the weather station at the experimental site were used. If these data were not available, then data from the adjacent

weather station in the China Meteorological Administration (CMA, http://www.data.cma.cn) were adapted by referring to the reported average or maximum values (Table S15, Text S1).

The necessary inputs of surface soil properties at the individual upland sites for the modified model were derived from Li et al. (2019), whereas those at the individual rice paddy sites are shown in Table S26. If the observed surface soil properties were not available, then the values were provided using the methods of Li et al. (2019). The soil clay and sand fraction and pH in the deep layers were set to be consistent with those in the surface soil. Depending on the SOC at the surface soil, the modified CNMM-DNDC calculated the SOC in the deep layers using the algorithms involved in Li (2016), and the BD in the deep layers were estimated using the SOC value in the corresponding layers based on the algorithms shown in Li (2016). Other soil properties (e.g., field capacity, wilting point and saturated hydraulic conductivity) were estimated using the pedo-transfer functions of Li et al. (2019).

The CNMM-DNDC contains a library of crop parameters. However, to ensure the normal growth of the crop(s), the model's default values for the crop TDD at the individual sites were adapted by the multiyear (at least five years) average of the sums of daily air temperatures during the growing season.

Agricultural management practice information included in the CNMM-DNDC input was organized on a daily scale. The management practice information for the cases of cultivated uplands was derived from Li et al. (2019), whereas that for the cases of rice paddy fields is listed in Table S37. It is worth noting that the information input for the cases of rice paddy fields required the start and end dates of the individual flooding events accompanied by the corresponding pH and depth of floodwater as model inputs. The default value of the initial floodwater pH at all sites was set at 7.0 due to a lack of observations. The cases in DY, FQP and YT had reported floodwater depth observations, and the cases of CS without floodwater depth observations were arbitrarily set to the traditional floodwater depth (0.04 m) of the DY site, which was located in the same region. For the SZ cases without floodwater depth observations, given that no site is adjacent to the Pearl River Delta region where SZ is located, the floodwater depth of the SZ site was calculated at 0.075 m.

2.3.2 Model operation

To reduce the influences of initial model inputs, the model simulation consists of a spin-up period

361 conducted for at least five years (depending on the availability of the model inputs) and the

362 corresponding experimental period. The sources of the daily meteorological data for the spin-up period

363 and the following simulation for cultivated uplands and rice paddy field sites were derived from Li et

364 al. (2019) and listed in Table S48, respectively. The cases for model calibration were identified on the

365 basis of covering as many climate conditions, soil properties and management practices as possible.

366 Therefore, for the simulation of NH_3 from urea application on cultivated uplands and rice paddy fields,

367 26 typical cases of DBW, FQU, and QZ and 10 typical cases of DY, FQP, and SZ were used for model

368 calibration. Regarding the simulation of NH_3 from the ABC application on cultivated uplands and rice

369 paddy fields, 3 typical cases of DBW and YT and 1 typical DY case were conducted for model

370 calibration. The remaining 23 independent cases were provided for model validation.

371 **2.4 Sensitivity analysis**

372 Sensitivity analysis was adopted to investigate model inputs and improved parametersthe

373 regulating factors in the modified CNMM-DNDC that simulates NH_3 volatilization following fertilizer

374 application. U37 in QZ and P4 in CS were chosen as the baseline cases to assess the model's behavior

375 in simulating NH_3 volatilization from cultivated uplands and rice paddy fields, respectively. One reason

376 for this selection was that U37 and P4 were geographically located near the center of the region for

377 cultivated upland and rice paddy cases, respectively. Another reason was that the selected cases

378 implement general Chinese management practices. The authors altered only one item at a time by

379 maintaining the others constant. Meteorological variables (i.e., 3-hourly averages of T_{air} and W;

380 3-hourly totals of P and R during measurement periods of NH_3 volatilization), soil properties (i.e., soil

381 clay fraction, pH, SOC content and BD), and field management practices (i.e., water management

382 (irrigation water amount or depth of floodwater) and nitrogen fertilization type, dose and depth) were

383 involved in the this sensitivity test of model inputs. U37 in QZ and P4 in CS were chosen as the

384 baseline cases to assess the model's behavior in simulating NH_3 volatilization from uplands and rice

385 paddy fields, respectively. One reason for this selection was that U37 and P4 were geographically

386 located near the center of the region for upland and rice paddy cases, respectively. Another reason was

387 that the selected cases implement general Chinese management practices. The authors altered only one

388   ~~item at a time by maintaining the others constant.~~ The model input items of the 3-hourly average of W,

389   3-hourly totals of P and R during the measurement periods of NH_3 volatilization, as well as the soil

390   clay fraction, SOC content, nitrogen fertilization dose, and depth of floodwater, were altered~~increased~~

391   by a range from −30% to +30% with an interval of 10%. Soil BD and pH, with narrow amplitudes in

392   situ, were altered within the ranges of 1.17 to 1.47 (U37) and 0.89 to 1.19 (P4) with an interval of 0.05

393   and within the ranges of 7.3 to 8.9 (U37) and 6.2 to 8.1 (P4) with an interval of 0.3, respectively. The

394   3-hourly average T_{air} during the measurement period of NH_3 volatilization was altered within the range

395   of −3 ℃ to +3 ℃ with an interval of 1 ℃. The irrigation water amount and nitrogen fertilization depth

396   and type were set as 0.2/0.5/5 cm, 5/10/15 cm and ABC/ammonium-based nitrogen (N) fertilizers

397   excluding ABC, respectively. The corresponding baselines and lower/upper bounds of the above ~~items~~

398   model inputs involved in the sensitivity analysis are listed in Table S~~5~~9. In addition, the parameters

399   added and revised for simulating NH_3 volatilization from cultivated uplands were involved in the

400   sensitivity analysis of improved parameters, including f_{SM} and f_T in the process of urea hydrolysis, f_{Ts_ABC}

401   in the process of ABC decomposition, and f_{temp}, f_{clay}, f_{water}, f_{depth}, f_{canopy} and f_{rain} in the process of liquid

402   NH_3 volatilization. The parameters in Eq. (3) for simulating NH_3 volatilization from rice paddy fields

403   were involved in the sensitivity analysis of improved parameters, including k_d, k_a and k_{vN}. And f_{alg}, a

404   newly introduced factor effect on floodwater pH, was also involved in the sensitivity analysis of

405   improved parameters for simulating NH_3 volatilization from rice paddy fields. In each sensitivity

406   analysis, an improved parameter was altered by a range from −30% to +30% by an interval of 10%,

407   with the others remaining constant. The sensitivity analysis of f_{Ts_ABC} was conducted at U4 case in QZ

408   with ABC application. The change ratios of cumulative NH_3 volatilization during the measurement

409   periods between the lower/upper and baseline simulations were applied as the quantitative evaluation

410   index for the sensitivity analysis (Abdalla et al., 2020).

411   **2.5 Evaluation of model performance and statistical analysis**

412   The index of agreement (IA), Nash–Sutcliffe Index (NSI), relative model bias (RMB), as well as

413   slope, significance level and coefficient of determination (R^2) of the zero-intercept linear regression

414   (ZIR) between the observed (O) and simulated (S) values were applied to quantitatively assess the

performance of the original and modified models. The algorithms of these statistical metrics refer to Li et al. (2019). If the slope and R^2 of the zero-intercept linear regression as well as the IA and NSI values are closer to 1, then the model performance is better. The SPSS Statistics Client 19.0 (SPSS Inc., Chicago, USA) software package was used for the multiple regression analysis. The Origin 8.0 (OriginLab Ltd., Guangzhou, China) software package was used for graph drawing.

3. Results

3.1 Ammonia volatilization from cultivated uplands

The observed cumulative ~~ammonia~~NH$_3$ volatilization (CAV) in all the cases of ~~the~~ cultivated uplands during the measurement periods totaled 0.6–127.7 kg N ha^{-1} (mean: 27.5 kg N ha^{-1}). The corresponding CAVs simulated by the original and modified CNMM-DNDC totaled 0.5–94.1 kg N ha^{-1} (mean: 33.2 kg N ha^{-1}) and 0.8–115.2 kg N ha^{-1} (mean: 27.8 kg N ha^{-1}), respectively (Table S~~6~~4). The original CNMM-DNDC performed poorly in simulating all the observed cumulative NH$_3$ volatilization cases, showing an acceptable IA (0.55), an unacceptable NSI (–1.49) and an insignificant ZIR (slope = 1.11 and $R^2 = 0.06$) (data not shown).

In this study, several modifications were conducted to improve the CNMM-DNDC performance in simulating NH$_3$ volatilizations from ~~upland soils.~~cultivated uplands. Regarding either the typically calibrated or independently validated cases, the modified CNMM-DNDC did not perform well in simulating daily NH$_3$ fluxes, with low IA and unacceptable NSI values (Table 3). This result was probably because the simulated NH$_3$ dynamic peak time could not absolutely be matched to the observed peak time, although the modified model captured the observed NH$_3$ dynamic trend. For the 3 only typically calibrated ABC cases, the modified model performed marginally well in simulating CAVs, showing a good IA (0.75) but a low NSI (0.14) and an insignificant ZIR ($R^2 = 0.64$) (Table 3). However, the modified model showed a perfect performance in simulating CAVs of both the calibrated and validated urea cases, with IA values (0.93 and 0.91) close to 1, acceptable NSI values (0.73 and 0.49), and significant ZIRs ($R^2 = 0.71$ with slope = 0.94 and $R^2 = 0.74$ with slope = 1.06) (Table 3). Regarding the CAVs of all the individual cases of cultivated uplands, the modified model reported an |RMB| of 1.0–307.8% (mean: 69.8%, Table 2), with only 16% (seven of forty-four) of cases suffering

442   from an |RMB| larger than 100%.

3.2 Ammonia volatilization from rice paddy fields

444   Figure 3, 4 and 5 illustrated the observed and simulated NH_3 volatilization and auxiliary variables

445   (e.g., temperatures, pH and NH_4^+ concentrations of floodwater) in each rice paddy case. The cases with

446   the same observed variables were associated in a figure for unified formatting. The observed CAVs in

447   all cases of rice paddy fields (2 and 17 cases for ABC and urea applications, respectively) during the

448   measurement periods totaled 5.9–39.8 kg N ha^{-1} (mean: 18.1 kg N ha^{-1}, Table 2), with fertilizer

449   application doses of 40.5–162.2 kg N ha^{-1} (mean: 81.4 kg N ha^{-1}). Given the lack of the capacity to

450   simulate the water-flooded layer over rice paddy fields, the original CNMM-DNDC could not simulate

451   NH_3 volatilizations from rice paddy fields. The corresponding CAVs simulated by the modified

452   CNMM-DNDC totaled 3.4–39.1 kg N ha^{-1} (mean: 16.2 kg N ha^{-1}, Table 2). Regarding the CAVs of all

453   the individual cases of rice paddy fields, the modified model demonstrated an |RMB| of 0.3–94.9%

454   (mean: 32.7%, Table 2), and none of nineteen cases showed an |RMB| larger than 100%. With regard to

455   the only two ABC cases, the simulated daily NH_3 fluxes generally matched the observations of the

456   typically calibrated and independently validated cases (P1 and P2, respectively), although the simulated

457   peak emissions of the first day for P1 were lower than the observations (Fig. 3e–f). For P1 and P2, the

458   corresponding statistical indices showed that IA values were 0.33 and 0.94, the NSI values were 0.02

459   and 0.85, and the ZIR slopes were 0.16 (not available R^2 and p values, $n = 7$) and 0.90 ($R^2 = 0.71$, not

460   significant, $n = 4$), respectively (Table 3). The observed and simulated daily NH_3 fluxes due to urea

461   application in the individual cases are illustrated in Fig. 4c–f and Fig.5i–k, respectively. As the figures

462   demonstrate, the temporal NH_3 flux variation pattern simulated by the modified model generally

463   followed that observed in the field. Regarding the simulations of the 10 typically calibrated and 7

464   independently validated urea cases, the modified model did not show good performance in terms of the

465   daily NH_3 flux, with IA values of 0.53 and 0.72, NSI values of –0.35 and 0. 36 and ZIR slopes of 0.47

466   ($R^2 = 0.04$, $p < 0.05$, $n = 176$) and 0.56 ($R^2 = 0.19$, $p < 0.001$, $n = 63$), respectively (Table 3). However,

467   the modified CNMM-DNDC performed extremely well in simulating CAVs of the calibrated and

468   validated urea cases, showing good IA values of 0.88 and 0.85, acceptable NSI values of 0.30 and 0.60,

469 and significant ZIR slopes of 1.03 ($R^2 = 0.68$, $n = 10$) and 0.77 ($R^2 = 0.65$, $n = 7$), respectively (Table

470 3).

471 ~~As Fig. 6 shows, with regard to the simulations of all 40 typically calibrated and 23 independently~~

472 ~~validated cases of uplands and rice paddy fields by the modified model, significant zero-intercept linear~~

473 ~~relationships between the simulated and observed CAVs were found, with slopes of 0.94 ($R^2 = 0.76$)~~

474 ~~and 0.98 ($R^2 = 0.71$), respectively. In general, the above results indicated that the modifications made in~~

475 ~~this study obviously improved the performance of the CNMM-DNDC in simulating NH$_3$ volatilization~~

476 ~~following applications of synthetic nitrogen fertilizers to upland and rice paddy soils.~~

477 **3.3 Model performance in terms of other auxiliary variables in rice paddy fields**

478   Table 4 lists the statistical indices used to evaluate the performance of the modified

479 CNMM-DNDC in the simulation of floodwater temperatures, pH values and NH_4^+ concentrations when

480 the model was calibrated and validated. The modified model generally captured the trends in

481 floodwater temperature (Fig. 5a–b), although the simulated floodwater temperatures of several certain

482 days for P9 were lower than the observations. The modified CNMM-DNDC, which introduced the

483 effect of algal growth on floodwater pH, generally simulated the observed daily elevated floodwater pH

484 resulting from algal photosynthetic activity (Fig. 3a–b and Fig. 5c–e). The simulation of calibrated (P1,

485 P9 and P10, Fig. 3a and Fig. 5c–d) and validated cases (P2 and P19, Fig. 3b and Fig. 5e) of floodwater

486 pH resulted in good IA values of 0.83 and 0.79, acceptable NSI values of 0.55 and 0.36, and ZIRs with

487 significant R^2 values of 0.55 (slope = 1.00, $n = 147$) and 0.36 (slope = 1.01, $n = 45$), respectively. The

488 simulated and observed daily NH_4^+ concentrations in the floodwater of the ABC and urea cases are

489 illustrated in Fig. 3c–d, Fig. 4a–b and Fig. 5f–h. Compared to the observed floodwater NH_4^+

490 concentrations of the ABC cases, the model simulation underestimated the peak concentration on the

491 first day after ABC application for the P1 case but captured the peak concentration of the P2 case (Fig.

492 3c–d). The modified CNMM-DNDC generally captured the observed temporal pattern in the daily

493 NH_4^+ concentrations during the observation periods following urea application, although discrepancies

494 existed in the magnitudes of some cases; e.g., the model overestimated the floodwater NH_4^+

495 concentration in the P7 and P8 cases (Fig. 4a–b) and underestimated that in the P6 (Fig. 4b) and P19

cases (Fig. 5h). Significant ZIRs between the simulated and observed daily floodwater NH_4^+

concentrations of the typically calibrated and independently validated cases yielded significant slopes

of 1.03 ($R^2 = 0.48$, $n = 24$) and 0.74 ($R^2 = 0.34$, $n = 55$), the IA values were 0.78 and 0.68, and the NSI

values were 0.48 and 0.25, respectively (Table 4).

3.4 Summary for the performance of CNMM-DNDC in simulating NH_3 volatilization

To sum up, Aas Fig. 6 shows, with regard to the simulations of all 40 typically calibrated and 23

independently validated cases of cultivated uplands and rice paddy fields by the modified model,

significant zero-intercept linear relationships between the simulated and observed CAVs were found,

with slopes of 0.94 ($R^2 = 0.76$) and 0.98 ($R^2 = 0.71$), respectively. In general, the above results

indicated that the modifications made in this study obviously improved the performance of the

CNMM-DNDC in simulating NH_3 volatilization following applications of synthetic nitrogen fertilizers

to cultivated upland and rice paddy soils. Nevertheless, the simulated CAV from cultivated upland

cases with fertilizer application depth (U6, U20 and U44) and irrigation/precipitation (U16, U22 and

U26) by the modified model resulted in the RMB larger than 150%. With regard to the cases in the rice

paddy fields, the simulations of the modified model with an absolute value of RMB larger than 50%

occurred in P1, P9 and P13 cases. The modified model resulted in the largest RMB of 94.9% between

the observed and simulated CAV occurred in the urea case of P9 which was located in DY under cloudy

conditions. The ABC case of P1 with RMB of –57% suffered from a seriously underestimation of NH_4^+

concentration in the floodwater (Fig. 3). For the cases in SZ, the modified CNMM-DNDC generally

underestimated NH_3 volatilization from the almost all cases with low N dose, but overestimated NH_3

volatilization from the cases with high N dose.

**3.45 Sensitivity Regulating factors of model inputs and improved parameters the modified model
in simulating NH_3ammonia volatilization**

The sensitivity analysis of model input items indicated that NH_3 volatilization from cultivated

uplands soils was primarily regulated by field management practices (Fig. 7a). The changes in N dose,

the different N types and the implementation of irrigation had considerable effects on NH_3

volatilization from cultivated uplands soils. In addition, a fertilization depth of 15 cm resulted in a –23%

change in NH_3 volatilization, and the increase in irrigation amount had an inhibitory effect on NH_3

volatilization. Moreover, in comparison to other soil properties, the changes in soil SOC had a greater

influence (–19% to 16%) on NH_3 volatilization. Among all considered meteorological variables, NH_3

volatilization from cultivated uplands soils appeared to be the most sensitive response to changes in air

temperature (Fig. 7a). However, NH_3 volatilization from rice paddy soils was sensitive to changes in

fertilization and floodwater management, which increased with N dosage and decreased with the depth

of fertilizer application and that of floodwater (Fig. 7b). For all soil variables considered in the

sensitivity analysis, only the changes in soil pH had a great influence on NH_3 volatilization from rice

paddy soils.fields. In addition, NH_3 volatilization from rice paddy soils decreased with solar radiation.

With regard to the sensitivity analysis of the improved parameters, NH_3 volatilization from cultivated

uplands showed more sensitive to the reduction of the improved parameters than to the increase of

those. Generally, as the improved parameters reduced, NH_3 volatilization from cultivated uplands

decreased. Moreover, NH_3 volatilization from rice paddy fields displayed complicated response to the

change of the improved parameters involved in the process of NH_3 volatilization from rice paddy fields.

For instance, no matter whether k_a increased or reduced, NH_3 volatilization trend to decrease while NH_3

volatilization increased with the increasing of k_d. The above results indicated that the modifications in

simulating NH_3 volatilization from either cultivated uplands or rice paddy fields were effective and

feasible.

4. Discussion

4.1 Model performance in simulating Factors affecting NH_3ammonia volatilization from cultivated uplands

NH_3 volatilization from soil-plant upland systems is an extremely complex process (Freney and Simpson, 1983; Sommer et al., 2004). The mechanism of NH_3 volatilization in the modified

CNMM-DNDC is mainly inherited from that in the DNDC model modified by Li et al. (2019). The

simulated rate of NH_3ammonia flux is jointly determined by the regulating factors of wind speed, soil

depth, clay fraction, soil temperature, soil moisture, vegetation canopy, and rainfall-induced canopy

wetting. ~~It is obvious that soil properties play an important role in regulating NH_3 volatilization from upland soils, as has been reported by a great number of studies (e.g., Duan and Xiao, 2000; Lei et al., 2017; Martens and Bremner, 1989). In addition, a~~We found that the complicated management practices bring obstacles to modeling. ~~A~~cross all the cases of cultivated uplands (Table S~~6~~4), the simulations of the modified CNMM-DNDC with an RMB larger than 150% occurred in the cases with fertilizer application depth (U6 with broadcast followed by tillage (BFT) 20 cm, U20 with BFT 5 cm and U44 with deep point placement 5–10 cm) and irrigation/precipitation (U16 with 4–6 cm irrigation, U22 with 4–6 cm irrigation and U26 with 0.8 cm irrigation and 3.69 cm precipitation). ~~Compared with~~ Among ~~all~~ the all cases with fertilizer application depth or irrigation/precipitation (including 38 cases), the proportion of the cases with RMB greater than 150% ~~(6 cases)~~ accounted for 16% (6 cases). This result might be because the model could not simulate well the inhibition mechanisms of some situations of fertilization depth and water-adding events effect on NH_3 volatilization. Moreover, Li et al. (2019) also reported that irrigation/precipitation during the measurement periods had a complex effect (e.g., reduction and stimulation) on NH_3 volatilization following nitrogen fertilizer application in cultivated upland~~s soils~~, and determining this information is still a considerable challenge in NH_3 simulations by biogeochemical models. At the same time, Li et al. (2019) also found that the doses and depths of the fertilizer applications jointly accounted for 43% ($p < 0.001$) of the variance in the observed CAVs. The results demonstrated that the simulated NH_3 volatilization from cultivated uplands following nitrogen fertilizer application accompanied with deep- or mixed-placement or irrigation/precipitation by the modified model still had some deviation from the observations, and more synchronous observations of NH_3 volatilization and other auxiliary variables (e.g., soil moisture, NH_4^+ concentration and nitrogen uptake by crops) in these situations are urgently needed to further revise the CNMM-DNDC.

4.2 Model performance in simulating NH_3 volatilization from rice paddy fields

In this study, four improvements in the pH of floodwater were involved in the modified CNMM-DNDC. First, floodwater over rice paddy soil was added, which enabled the simulation of floodwater pH in the modified model. Second, the modified model used the initial pH of floodwater and the pH of the surface soil to calculate the floodwater pH. The above two improvements allowed the

introduction of the J-M model into the modified CNMM-DNDC. The present relatively reliable biogeochemical models rarely involve floodwater over rice paddy soil when simulating NH_3 volatilization from rice paddy fields, which is not in accordance with the natural state. Third, when urea was applied to the surface floodwater, the subsequent urea hydrolysis reaction could increase the floodwater pH, and this process was added to the modified model by referring to the algorithms applied in the original model for upland soils soils (Sec. 2.21.2). Finally, the effect of algal growth on floodwater pH was introduced into the modified model by calculating the ratio of the solar shortwave radiation effect on algal photosynthesis. In detail, under cloudy conditions in DY (P9), only 9% of the applied urea-N was observed to be lost as NH_3ammonia from the rice paddy soil, while up to 40% of the applied urea-N was observed to be lost under high solar radiation conditions in YTA (P19) (Cai et al., 1992). However, the modified CNMM-DNDC overestimated the emissions from DY but underestimated those from YTA, which could be attributed to the overestimation of the pH during the first three observation days in DY and the underestimation of NH_4^+ concentrations in YTA (Fig. 5). In addition, algal blooms only appeared on the surface of calm water; thus, a number of factors, such as irrigation, heavy rain, strong wind, and drainage, could hamper the growth of algae (Cao et al., 2013). Due to the basal dressing followed by irrigation (Gong et al., 2013), which inhibited the reproduction of algae in SZ (P11 and P12 cases), the observed NH_3ammonia emissions accounted for only 10%−13% of the applied nitrogen. Unfortunately, the aforementioned factors that reduced algal growth were not introduced into the modified CNMM-DNDC because of limited reports, which resulted in an overestimation of NH_3ammonia emissions of 6.4 and 2.6 kg N ha^{-1} for P11 and P12 in SZ cases with a high rate of urea application, respectively. Therefore, mMore observational data on the effect of algal growth on floodwater pH and subsequent NH_3 volatilization are needed to improve the simulation of the modified model on NH_3 volatilization from rice paddy fields. Therefore, compared to the model without floodwater, the modified CNMM-DNDC with the introduction of a floodwater layer, as well as the corresponding processes, into the simulation of NH_3 volatilization provided a more scientific algorithm for the simulation of NH_3 loss from rice paddy fields, thereby enabling the simulation of the pH and NH_4^+ concentration of floodwater. However, the depth of surface floodwater was kept at a constant value (such as the average depth of the floodwater) for each flooding event in the modified model, but

this operation was inconsistent with the field states. The floodwater depth actually changed with real-time evaporation and precipitation. Therefore, a module for calculating the dynamics of floodwater depth driven by real-time evaporation and precipitation is needed to better simulate the effect of floodwater depth on NH_3 volatilization. The results of this study suggest that accurate field measurements and a corresponding reliable simulation of floodwater depth are crucial for the simulation of NH_3 volatilization by the modified CNMM-DNDC.

4.2 Effects of floodwater on ammonia volatilization from rice paddy fields

Floodwater pH has been considered one of the primary factors affecting NH_3 volatilization from rice paddy fields (Fillery et al., 1984; Hayashi et al., 2006; Jayaweera and Mikkelsen, 1991). As floodwater pH increases, the equilibrium of NH_4^+ ions and $NH_{3(aq)}$ in floodwater transfers in the direction of $NH_{3(aq)}$ formation, which will increase the potential for subsequent NH_3 volatilization (Jayaweera and Mikkelsen, 1990a; Sommer et al., 2004). In this study, four improvements in the pH of floodwater were involved in the modified CNMM-DNDC. First, floodwater over rice paddy soil was added, which enabled the simulation of floodwater pH in the modified model. Second, the modified model used the initial pH of floodwater and the pH of the surface soil to calculate the floodwater pH. The above two improvements allowed the introduction of the J-M model into the modified CNMM-DNDC. The present relatively reliable biogeochemical models rarely involve floodwater over rice paddy soil when simulating NH_3 volatilization from rice paddy fields, which is not in accordance with the natural state. Third, when urea was applied to the surface floodwater, the subsequent urea hydrolysis reaction could increase the floodwater pH, and this process was added to the modified model by referring to the algorithms applied in the original model for upland soils (See. 2.2.2). Finally, the effect of algal growth on floodwater pH was introduced into the modified model by calculating the ratio of the solar shortwave radiation effect on algal photosynthesis. In detail, under cloudy conditions in DY (P9), only 9% of the applied urea-N was observed to be lost as ammonia from the rice paddy soil, while up to 40% of the applied urea N was observed to be lost under high solar radiation conditions in YTA (P19) (Cai et al., 1992). However, the modified CNMM-DNDC overestimated the emissions from DY but underestimated those from YTA, which could be attributed to the overestimation of the pH

during the first three observation days in DY and the underestimation of NH_4^+ concentrations in YTA (Fig. 5). In addition, algal blooms only appeared on the surface of calm water; thus, a number of factors, such as irrigation, heavy rain, strong wind, and drainage, could hamper the growth of algae (Cao et al., 2013). Due to the basal dressing followed by irrigation (Gong et al., 2013), which inhibited the reproduction of algae in SZ (P11 and P12 cases), the observed ammonia emissions accounted for only 10%–13% of the applied nitrogen. Unfortunately, the aforementioned factors that reduced algal growth were not introduced into the modified CNMM-DNDC because of limited reports, which resulted in an overestimation of ammonia emissions of 6.4 and 2.6 kg N ha^{-1} for P11 and P12 in SZ cases with a high rate of urea application, respectively. Previous studies have also shown that the stimulation of NH_3 volatilization from rice paddy fields is affected by algal growth, which largely contributes to the elevation of floodwater pH resulting from algal photosynthetic activity (Buresh et al., 2008; Fillery and Vlek, 1986; Mikkelsen et al., 1978). The addition of a suitable photosynthetic inhibitor also controlled the pH of the floodwater, implying that the increase in pH was caused by algal growth (Bowmer and Muirhead, 1987). Therefore, more observational data on the effect of algal growth on floodwater pH and subsequent NH_3 volatilization are needed to improve the simulation of the modified model on NH_3 volatilization from rice paddy fields.

Many studies have found that the depth of surface floodwater has a substantial influence on NH_3 volatilization (Fillery et al., 1984; Freney et al., 1988; Hayashi et al., 2006). The sensitivity analysis of this study also indicated that NH_3 volatilization from rice paddy fields was sensitive to changes in the depth of surface floodwater (Fig. 7b). Jayaweera and Mikkelsen (1990b) demonstrated that the volatilization rate of NH_3 decreases as the depth of floodwater increases despite the small difference in meteorological factors and soil physicochemical properties. The reducing effects might be attributed to the following mechanisms. First, with increasing floodwater depth, the concentration of NH_4^+ in floodwater decreases (Cai et al., 1986). Many studies have found that a lower concentration of NH_4^+ in floodwater contributes to the reduced potential of NH_3 volatilization in paddy fields (Bhagat et al., 1996; Hayashi et al., 2006; He et al., 2014; Liu et al., 2015; Song et al., 2004). Observations based on wind tunnel experiments showed that the NH_3 loss decreased from 14.6 mg L^{-1} to 4.5 mg L^{-1} as the depth of floodwater increased from 6.4 cm to 21.3 cm, while other environmental conditions were

4.3 Differences between NH_3 volatilization from cultivated uplands and rice paddy fields

NH$_3$ volatilization from soil-plant upland systems is an extremely complex process (Freney and Simpson, 1983; Sommer et al., 2004). It is obvious that soil properties play an important role in regulating NH_3 volatilization from cultivated uplands, as has been reported by a great number of studies (e.g., Duan and Xiao, 2000; Lei et al., 2017; Martens and Bremner, 1989). In addition, NH_3 volatilization from cultivated uplands was simultaneously regulated by the complicated management practices. As the sensitivity analysis indicated, NH_3 volatilization from cultivated uplands was primarily regulated by the dose, type and application depth of N fertilizer and water management (Fig. 7a). With regard to NH_3 volatilization from rice paddy fields , floodwater pH has been considered one of the primary factors affecting NH_3 volatilization from rice paddy fields (Fillery et al., 1984; Hayashi et al., 2006; Jayaweera and Mikkelsen, 1991). As floodwater pH increases, the equilibrium of NH_4^+ ions and $NH_{3(aq)}$ in floodwater transfers in the direction of $NH_{3(aq)}$ formation, which will increase the potential for subsequent NH_3 volatilization (Jayaweera and Mikkelsen, 1990a; Sommer et al., 2004). Previous studies have also shown that the stimulation of NH_3 volatilization from rice paddy fields is

688 affected by algal growth, which largely contributes to the elevation of floodwater pH resulting from algal

689 photosynthetic activity (Buresh et al., 2008; Fillery and Vlek, 1986; Mikkelsen et al., 1978). The

690 addition of a suitable photosynthetic inhibitor also controlled the pH of the floodwater, implying that the

691 increase in pH was caused by algal growth (Bowmer and Muirhead, 1987). In addition, ~~M~~many studies

692 have found that the depth of surface floodwater has a substantial influence on NH_3 volatilization

693 (Fillery et al., 1984; Freney et al., 1988; Hayashi et al., 2006). The sensitivity analysis of this study also

694 indicated that NH_3 volatilization from rice paddy fields was sensitive to changes in the depth of surface

695 floodwater (Fig. 7b). Jayaweera and Mikkelsen (1990b) demonstrated that the volatilization rate of

696 NH_3 decreases as the depth of floodwater increases despite the small difference in meteorological

697 factors and soil physicochemical properties. The reducing effects might be attributed to the following

698 mechanisms. First, with increasing floodwater depth, the concentration of NH_4^+ in floodwater decreases

699 (Cai et al., 1986). Many studies have found that a lower concentration of NH_4^+ in floodwater

700 contributes to the reduced potential of NH_3 volatilization in paddy fields (Bhagat et al., 1996; Hayashi

701 et al., 2006; He et al., 2014; Liu et al., 2015; Song et al., 2004). Observations based on wind-tunnel

702 experiments showed that the NH_3 loss decreased from 14.6 mg L^{-1} to 4.5 mg L^{-1} as the depth of

703 floodwater increased from 6.4 cm to 21.3 cm, while other environmental conditions were similar

704 (Jayaweera et al., 1990). Second, a reduction in the depth of floodwater increases the volatilization rate

705 constant of $NH_{3(aq)}$ (k_{vN}), thus increasing NH_3 volatilization from floodwater.

706 According to the above results, the regulatory factors affecting NH_3 volatilization from rice paddy

707 fields were demonstrated to be different from those from cultivated uplands, which was also supported

708 by previous research (Tian et al., 2001; Zhao et al., 2009). NH_3 volatilization from cultivated uplands

709 was primarily influenced by the regulatory factors of soil properties and field management practices.

710 However, given the existence of floodwater over rice paddy field soils, NH_3 volatilization from rice

711 paddy fields was additionally affected by flooding management strategies, such as floodwater pH and

712 depth. Therefore, the mechanisms and algorithms applied in simulating NH_3 volatilization from

713 cultivated uplands are not appropriate for simulating NH_3 volatilization from rice paddy fields. In the

714 modified CNMM-DNDC, NH_3 volatilization following nitrogen fertilizer application in cultivated

715 upland~~s soils~~ was based on first-order kinetics. However, the modified CNMM-DNDC adopted the J-M

model, which was based on the two-film theory of mass transfer, to calculate NH_3 volatilization following nitrogen fertilizer application in rice paddy field soils. The results suggest that the application of two different mechanisms according to the distinguished properties of cultivated uplands and rice paddy fields to simulate NH_3 volatilization is necessary for process-based biogeochemical models, such as the CNMM-DNDC used in this study.

~~5.~~ Conclusions

The Catchment Nutrient Management Model-DeNitrification-DeComposition ~~simulation of ammonia (NH₃) volatilization in the~~ (CNMM-DNDC) model was evaluated and modified based on 44 and 19 field observation cases of ammonia (NH₃) volatilization following synthetic fertilizer application events in cultivated uplands and rice paddy fields in China, respectively. The original CNMM-DNDC performed poorly in terms of simulating the observed NH_3 volatilizations from cultivated uplands ~~soils~~, and it failed to simulate NH_3 volatilization from rice paddy fields because it could not simulate the water-flooded layer over the rice paddy field. The mechanisms of NH_3 volatilization from cultivated uplands and rice paddy fields are different due to the existence of floodwater over rice paddy soils. Therefore, separate modules simulating NH_3 volatilization from uplands and rice paddy fields were developed. The primary modifications for simulating NH_3 volatilization from cultivated uplands ~~soils~~ were mainly adopted from Li et al. (2019), and NH_3 volatilization from cultivated uplands ~~soils~~ are regulated by meteorological conditions, soil properties and crop statuses. ~~In addition, to solve the problem of the simulation deviation derived from different time steps, a time step parameter was introduced and calibrated.~~ With regard to the simulation of NH_3 volatilization from rice paddy fields, four major modifications were performed in this study. First, floodwater over rice paddy soil, as well as the simulation of floodwater pH, was added to the module simulating NH_3 volatilization from rice paddy fields. Second, the Jayaweera-Mikkelsen model was newly introduced into the modified CNMM-DNDC to calculate NH_3 volatilization from rice paddy fields. Third, the effect of algal growth on floodwater pH was newly parameterized and added into the model. Finally, the parameters corresponding to NH_3 volatilization following ammonium bicarbonate application were calibrated. The modified model provided an excellent performance in simulating NH_3

volatilization following synthetic nitrogen fertilizer applications to either cultivated uplands or rice paddy fields. The sensitivity analysis demonstrated that NH_3 volatilization from cultivated uplands was principally regulated by soil properties and field management practices while fertilizer application and flooding management strategies, such as floodwater pH and depth, played a major role in regulating NH_3 volatilization from rice paddy fields. ~~Nevertheless, the simulated NH_3 volatilization following nitrogen fertilizer application by the modified model still had some deviations from the observations, when deep- or mixed placement or irrigation/precipitation were accompanied with the fertilizer event in upland soils and when simulating and limiting factors on algal growth occurred with fertilizer events in rice paddy fields. A further revision to the modified model is still needed in future studies to overcome these deficiencies. Nevertheless, the modified CNMM-DNDC is acceptable for regional or national NH_3 simulations when developing strategies to alleviate environmental pollution and compile NH_3 emission inventories.~~

Data availability. All of the model output used to produce the figures can be obtained from the Supplement, and all of the observed data sets used in this study were collected from published peer-reviewed articles. The code and executive program of the modified model can be obtained from http://doi.org/10.6084/m9.figshare.19388756.

Author contribution. XZ, YL, and WZ contributed to developing the idea and methodology of this study. SL arranged the research data, improved and implemented the model simulation, prepared the paper with contributions from all co-authors. RW, KW, and CZ contributed to collect and maintained the research data. SH, CL, and ZY analyzed study data and verified the results.

Competing interests. The authors declare that they have no conflict of interest.

765 *Acknowledgments.* This work was supported by the Chinese Academy of Sciences (grant numbers:
766 ZDBS-LY-DQC007), the National Natural Science Foundation of China (grant numbers: 41907280)
767 and the China Postdoctoral Science Foundation (grant numbers: 2019M650808).

References

769 Abdalla, M., Song, X., Ju, X., Topp, C. F. E., Smith, P.: Calibration and validation of the DNDC model to

770 estimate nitrous oxide emissions and crop productivity for a summer maize-winter wheat double

771 cropping system in Hebei, China, Environ. Pollut., 262, doi:10.1016/j.envpol.2020.114199, 2020.

772 Alberty, R. A.: Physical chemistry, John Wiley & Sons, New York, 1983.

773 Anderson, D. M., Burkholder, J. M., Cochlan, W. P., Glibert, P. M., Gobler, C. J., Heil, C. A., Kudela, R.

774 M., Parsons, M. L., Rensel, J. E. J., Townsend, D. W., Trainer, V. L., Vargo, G. A.: Harmful algal blooms

775 and eutrophication: Examining linkages from selected coastal regions of the United States, Harmful

776 Algae, 8, 39–53, doi:10.1016/j.hal.2008.08.017, 2008.

777 Behera, S. N., Sharma, M., Aneja, V. P., Balasubramanian, R.: Ammonia in the atmosphere: a review on

778 emission sources, atmospheric chemistry and deposition on terrestrial bodies, Environ. Sci. Pollut. R., 20,

779 8092–8131, doi:10.1007/s11356-013-2051-9, 2013.

780 Bhagat, R. M., Bhuiyan, S. I., Moody, K.: Water, tillage and weed interactions in lowland tropical rice: a

781 review, Agr. Water Manage., 31, 165–184, doi:10.1016/0378-3774(96)01242-5, 1996.

782 Bobbink, R., Hornung, M., Roelofs, J. G. M.: The effects of air-borne nitrogen pollutants on species

783 diversity in natural and semi-natural European vegetation, J. Ecol., 86, 717–738,

784 doi:10.1046/j.1365-2745.1998.8650717.x, 1998.

785 Bouwman, A. F., Lee, D. S., Asman, W. A. H., Dentener, F. J., VanderHoek, K. W., Olivier, J. G. J.: A

786 global high-resolution emission inventory for ammonia, Global Biogeochem. Cy., 11, 561–587,

787 doi:10.1029/97gb02266, 1997.

788 Bowmer, K. H., Muirhead, W. A.: Inhibition of algal photosynthesis to control pH and reduce ammonia

789 volatilization from rice floodwater, Fertil. Res., 13, 13–29, doi:10.1007/BF01049799, 1987.

790 Buresh, R., Ramesh Reddy, K. and van Kessel, C.: Nitrogen Transformations in Submerged Soils, In:

791 Raun, J.S.S.a.W.R. editor, Nitrogen in Agricultural Systems, 401–436, 2008.

792 Cai, G., Peng, G., Wang, X., Zhu, J.: Ammonia volatilization from urea applied to acid paddy soil in

793 southern china and its control, Pedosphere, 2, 345–354, 1992.

794 Cai, G., Zhu, Z., Trevitt, A., Freney, J. R., Simpson, J. R.: Nitrogen loss from ammonium bicarbonate

795 and urea fertilizers applied to flooded rice, Fertil. Res., 10, 203–215, doi:10.1007/BF01049350, 1986.

796 Cannavo, P., Recous, S., Parnaudeau, V., Reau, R.: Modeling N dynamics to assess environmental

797 impacts of cropped soils, Advances in Agronomy, 97, Academic Press, 131–174, 2008.

798 Cao, Y., Tian, Y., Yin, B., Zhu, Z.: Proliferation of algae and effect of its on fertilizer–N immobilization

799 in flooded paddy field, J. Plant Nutr. Fertil. Sc., 19, 111–116, doi:10.11674/zwyf.2013.0113, 2013.

800 Chien, S. H., Prochnow, L. I., Cantarella, H.: Chapter 8 Recent developments of fertilizer production and

801 use to improve nutrient efficiency and minimize environmental impacts, Advances in Agronomy, 102,

802 Academic Press, 267–322, 2009.

803 De Datta, S. K.: Nitrogen transformations in wetland rice ecosystems, Fertil. Res., 42, 193–203,

804 doi:10.1007/bf00750514, 1995.

805 Duan, Z., Xiao, H.: Effects of soil properties on ammonia volatilization, Soil Sci. Plant Nutr., 46,

806 845–852, 2000.

807 Dubache, G., Li, S., Zheng, X., Zhang, W., Deng, J.: Modeling ammonia volatilization following urea

808 application to winter cereal fields in the United Kingdom by a revised biogeochemical model, Sci. Total

809 Environ., 660, 1403–1418, doi:10.1016/j.scitotenv.2018.12.407, 2019.

810 Dutta, B., Congreves, K. A., Smith, W. N., Grant, B. B., Rochette, P., Chantigny, M. H., Desjardins, R. L.:

811 Improving DNDC model to estimate ammonia loss from urea fertilizer application in temperate

812 agroecosystems, Nutr. Cycl. Agroecosys., 106, 275–292, doi:10.1007/s10705-016-9804-z, 2016.

813 Felix, J. D., Elliott, E. M., Gish, T. J., McConnell, L. L., Shaw, S. L.: Characterizing the isotopic

814 composition of atmospheric ammonia emission sources using passive samplers and a combined

815 oxidation-bacterial denitrifier approach, Rapid Commun. Mass Sp., 27, 2239–2246,

816 doi:10.1002/rcm.6679, 2013.

817 Fillery, I. R. P., Simpson, J. R., Dedatta, S. K.: Influence of field environment and fertilizer management

818 on ammonia loss from flooded rice, Soil Sci. Soc. Am. J., 48, 914–920,

819 doi:10.2136/sssaj1984.03615995004800040043x, 1984.

820 Fillery, I. R. P., Vlek, P. L. G.: 4. Reappraisal of the significance of ammonia volatilization as an N loss

821 mechanism in flooded rice fields, Fertil. Res., 9, 79–98, doi:10.1007/BF01048696, 1986.

822 Freney, J. R., Simpson, J. R.: Gaseous loss of nitrogen from plant-soil systems, Developments in plant

823 and soil sciences, 9, 1983.

824 Freney, J. R., Trevitt, A. C. F., Muirhead, W. A., Denmead, O. T., Simpson, J. R., Obcemea, W. N.: Effect

825 of water depth on ammonia loss from lowland rice, Fertil. Res., 16, 97–107, doi:10.1007/bf01049767,

826 1988.

827 Giltrap, D., Saggar, S., Rodriguez, J., Bishop, P. :Modelling NH_3 volatilisation within a urine patch using

828 NZ-DNDC, Nutr. Cycl. Agroecosys., 108, 267–277, doi:10.1007/s10705-017-9854-x, 2017.

829 Gong, W., Zhang, Y., Huang, X., Luan, S.: High–resolution measurement of ammonia emissions from

830 fertilization of vegetable and rice crops in the Pearl River Delta Region, China, Atmos. Environ., 65,

831 1–10, doi:10.1016/j.atmosenv.2012.08.027, 2013.

832 Han, K., Zhou, C., Wang, L.: Reducing ammonia volatilization from maize fields with separation of

833 nitrogen fertilizer and water in an alternating furrow irrigation system, J. Integr. Agr., 13, 1099–1112,

834 doi:10.1016/s2095-3119(13)60493-1, 2014.

835 Hayashi, K., Nishimura, S., Yagi, K.: Ammonia volatilization from the surface of a Japanese paddy field

836 during rice cultivation, Soil Sci. Plant Nutr., 52, 545–555, doi:10.1111/j.1747-0765.2006.00053.x, 2006.

837 He, Y., Yang, S., Xu, J., Wang, Y., Peng, S.: Ammonia volatilization losses from paddy fields under

838 controlled irrigation with different drainage treatments, Sci. World J., doi:10.1155/2014/417605, 2014.

839 Holcomb III, J. C., Sullivan, D. M., Horneck, D. A., Clough, G. H.: Effect of irrigation rate on ammonia

840 volatilization, Soil Sci. Soc. Am. J., 75, 2341–2347, doi:10.2136/sssaj2010.0446, 2011.

841 Huang, X., Song, Y., Li, M., Li, J., Huo, Q., Cai, X., Zhu, T., Hu, M., Zhang, H.: A high-resolution

842 ammonia   emission   inventory   in   China,   Global   Biogeochem.   Cy.,   26,   GB1030,

843 doi:10.1029/2011gb004161, 2012.

844 Jayaweera, G. R., Mikkelsen, D. S.: Ammonia volatilization from flooded soil systems - a

845 computer-model.   I.   Theoretical   aspects,   Soil   Sci.   Soc.   Am.   J.,   54,   1447–1455,

846 doi:10.2136/sssaj1990.03615995005400050039x, 1990a.

847 Jayaweera, G. R., Mikkelsen, D. S.: Ammonia volatilization from flooded soil systems - a

848 computer-model.   II.   Theory   and   model   results,   Soil   Sci.   Soc.   Am.   J.,   54,   1456–1462,

849   doi:10.2136/sssaj1990.03615995005400050040x, 1990b.

850   Jayaweera, G. R., Mikkelsen, D. S.: Assessment of ammonia volatilization from flooded soil systems,

851   Adv. Agron., 45, 303–356, doi:10.1016/S0065-2113(08)60044-9, 1991.

852   Jayaweera, G. R., Paw U., K. T., Mikkelsen, D. S.: Ammonia volatilization from flooded soil systems: a

853   computer model. III. Validation of the model, Soil Sci. Soc. Am. J., 54, 1462–1468,

854   doi:10.2136/sssaj1990.03615995005400050041x, 1990.

855   Kong, L., Tang, X., Zhu, J., Wang, Z., Pan, Y., Wu, H., Wu, L., Wu, Q., He, Y., Tian, S., Xie, Y., Liu, Z.,

856   Sui, W., Han, L., Carmichael, G.: Improved inversion of monthly ammonia emissions in China based on

857   the Chinese ammonia monitoring network and ensemble Kalman filter, Environ. Sci. Technol., 53,

858   12529–12538, doi:10.1021/acsest.9b02701, 2019.

859   Lei, T., Guo, X., Ma, J., Sun, X., Feng, Y., Wang, H.: Kinetic and thermodynamic effects of moisture

860   content and temperature on the ammonia volatilization of soil fertilized with urea, Int. J. Agr. Biol. Eng.,

861   10, 134–143, doi:10.25165/j.ijabe.20171006.3232, 2017.

862   Li, C.: Biogeochemistry: Scientific fundamentals and modelling approach, Tsinghua University Press,

863   Beijing, 2016.

864   Li, C., Frolking, S., Frolking, T. A.: A model of nitrous-oxide evolution from soil driven by rainfall

865   events. 1. Model structure and sensitivity, J. Geophys. Res. - Atmos., 97, 9759–9776,

866   doi:10.1029/92jd00509, 1992.

867   Li, H., Han, Y., Cai, Z.: Modeling the ammonia volatilization from common urea and controlled releasing

868   urea fertilizers in paddy soil of Taihu region of China by Jayaweera–Mikkelsen model, Environ. Sci., 29,

869   1045–1052, doi:10.1007/BF01049507, 2008.

870   Li, S., Zheng, X., Zhang, W., Han, S., Deng, J., Wang, K., Wang, R., Yao, Z., Liu, C.: Modeling ammonia

871   volatilization following the application of synthetic fertilizers to cultivated uplands with calcareous soils

872   using an improved DNDC biogeochemistry model, Sci. Total Environ., 660, 931–946,

873   doi:10.1016/j.scitotenv.2018.12.379, 2019.

874   Li, Y., Schichtel, B. A., Walker, J. T., Schwede, D. B., Chen, X., Lehmann, C. M. B., Puchalski, M. A.,

875   Gay, D. A., Collett, J. L., Jr.: Increasing importance of deposition of reduced nitrogen in the United States,

876   P. Nat. Acad. Sci., USA 113, 5874–5879, doi:10.1073/pnas.1525736113, 2016.

877   Li, Y., Shen, J., Wang, Y., Gao, M., Liu, F., Zhou, P., Liu, X., Chen, D., Zou, G., Luo, Q., Ma, Q.: CNMM:

878   a grid-based spatially-distributed catchment simulation model, China Science Press, Beijing, 2017.

879   Liu, J., Ding, P., Zong, Z., Li, J., Tian, C., Chen, W., Chang, M., Salazar, G., Shen, C., Cheng, Z., Chen,

880   Y., Wang, X., Szidat, S., Zhang, G.: Evidence of rural and suburban sources of urban haze formation in

881   China: a case study from the Pearl River Delta region, J. Geophys. Res. - Atmos., 123, 4712–4726,

882   doi:10.1029/2017jd027952, 2018.

883   Liu, T., Fan, D., Zhang, X., Chen, J., Li, C., Cao, C.: Deep placement of nitrogen fertilizers reduces

884   ammonia volatilization and increases nitrogen utilization efficiency in no-tillage paddy fields in central

885   China, Field Crops Res., 184, 80–90, doi:10.1016/j.fcr.2015.09.011, 2015.

886   Liu, X., Ju, X., Zhang, F., Pan, J., Christie, P.: Nitrogen dynamics and budgets in a winter wheat–maize

887   cropping   system   in   the   North   China   Plain,   Field   Crops   Res.,   83,   111–124,

888   doi:10.1016/S0378-4290(03)00068-6, 2003.

889   Mariano, E., de Sant Ana Filho, C. R., Bortoletto-Santos, R., Bendassolli, J. A., Trivelin, P. C. O.:

890   Ammonia losses following surface application of enhanced-efficiency nitrogen fertilizers and urea,

891   Atmos. Environ., 203, 242–251, doi:10.1016/j.atmosenv.2019.02.003, 2019.

892   Martens, D. A., Bremner, J. M.: Soil properties affecting volatilization of ammonia from soils treated

893   with urea, Commun. Soil Sci. Plan., 20, 1645–1657, doi:10.1080/00103628909368173, 1989.

894   Martin, S. T., Hung, H. M., Park, R. J., Jacob, D. J., Spurr, R. J. D., Chance, K. V., Chin, M.: Effects of

895   the physical state of tropospheric ammonium-sulfate-nitrate particles on global aerosol direct radiative

896   forcing, Atmos. Chem. Phys., 4, 183–214, doi:10.5194/acp-4-183-2004, 2004.

897   Michalczyk, A., Kersebaum, K.C., Heimann, L., Roelcke, M., Sun, Q. P., Chen, X. P., Zhang, F. S.:

898   Simulating in situ ammonia volatilization losses in the North China Plain using a dynamic soil-crop

899   model, J. Plant Nutr. Soil Sc., 179, 270–285, doi:10.1002/jpln.201400673, 2016.

900   Mikkelsen, D. S., Datta, S. K. D., Obcemea, W. N.: Ammonia volatilization losses from flooded rice

901   soils, Soil Sci. Soc. Am. J., 42, 725–730, doi:10.2136/sssaj1978.03615995004200050043x, 1978.

902   Park, K. D., Lee, D. W., Li, Y., Chen, D., Park, C. Y., Lee, Y. H., Lee, C. H., Kang, U. G., Park, S. T., Cho,

903   Y. S.: Simulating ammonia volatilization from applications of different urea applied in rice field by

904   WNMM, Korean J. Crop Sci., 53, 8–14, 2008.

905 Paulot, F., Jacob, D. J., Pinder, R. W., Bash, J. O., Travis, K., Henze, D. K.: Ammonia emissions in the

906 United States, European Union, and China derived by high-resolution inversion of ammonium wet

907 deposition data: Interpretation with a new agricultural emissions inventory (MASAGE_NH$_3$), J.

908 Geophys. Res. - Atmos., 119, 4343–4364, doi:10.1002/2013jd021130, 2014.

909 Riddick, S., Ward, D., Hess, P., Mahowald, N., Massad, R., Holland, E.: Estimate of changes in

910 agricultural terrestrial nitrogen pathways and ammonia emissions from 1850 to present in the

911 Community Earth System Model, Biogeosciences, 13, 3397–3426, doi:10.5194/bg-13-3397-2016, 2016.

912 Roelcke, M., Li, S., Tian, X., Gao, Y., Richter, J.: In situ comparisons of ammonia volatilization from N

913 fertilizers in Chinese loess soils, Nutr. Cycl. Agroecosys., 62, 73–88, doi:10.1023/a:1015186605419,

914 2002.

915 Sanz-Cobena, A., Misselbrook, T., Camp, V., Vallejo, A.: Effect of water addition and the urease

916 inhibitor NBPT on the abatement of ammonia emission from surface applied urea, Atmos. Environ., 45,

917 1517–1524, doi:10.1016/j.atmosenv.2010.12.051, 2011.

918 Savard, M. M., Cole, A., Smirnoff, A., Vet, R.: δ^{15}N values of atmospheric N species simultaneously

919 collected using sector - based samplers distant from sources isotopic inheritance and fractionation,

920 Atmos. Environ., 162, 11–22, doi:10.1016/j.atmosenv.2017.05.010, 2017.

921 Schjørring, J. K.: Atmospheric ammonia and impacts of nitrogen deposition: Uncertainties and

922 challenges, New Phytol., 139, 59–60, doi:10.1046/j.1469-8137.1998.00173.x, 1998.

923 Sommer, S. G., Schjoerring, J. K., Denmead, O. T.: Ammonia emission from mineral fertilizers and

924 fertilized crops, In: Sparks, D.L. editor, Advances in Agronomy, 82, 557–622, 2004.

925 Song, Y., Fan, X., Lin, D., Yang, L., Zhou, J.: Ammonia volatilization from paddy fields in the Taihu lake

926 region and its influencing factors, Acta Pedologica Sinica, 265–269, doi:10.11766/trxb200306090216,

927 2004.

928 Tian, G., Cai, Z., Cao, J., Li, X.: Factors affecting ammonia volatilization from a rice–wheat rotation

929 system, Chemosphere, 42, 123–129, doi: 10.1016/S0045-6535(00)00117-X, 2001.

930 Vira, J., Hess, P., Melkonian, J., and Wieder, W. R.: An improved mechanistic model for ammonia

931 volatilization in Earth system models: Flow of Agricultural Nitrogen version 2 (FANv2), Geosci.

932 Model Dev., 13, 4459–4490, doi: 10.5194/gmd-13-4459-2020, 2020.

933   Wang, H., Hu, Z., Lu, J., Liu, X., Wen, G., Blaylock, A.: Estimation of ammonia volatilization from a

934   paddy field after application of controlled-release urea based on the modified Jayaweera-Mikkelsen

935   model combined with the Sherlock-Goh model, Commun. Soil Sci. Plan., 47, 1630–1643,

936   doi:10.1080/00103624.2016.1206120, 2016.

937   Xu, R., Tian, H., Pan, S., Prior, S. A., Feng, Y., Batchelor, W. D., Chen, J., Yang, J.: Global ammonia

938   emissions from synthetic nitrogen fertilizer applications in agricultural systems: Empirical and

939   process-based estimates and uncertainty, Global Change Biol., 25, 314–326, doi:10.1111/gcb.14499,

940   2019.

941   Zhan, X., Chen, C., Wang, Q., Zhou, F., Hayashi, K., Ju, X., Lam, S. K., Wang, Y., Wu, Y., Fu, J., Zhang,

942   L., Gao, S., Hou, X., Bo, Y., Zhang, D., Liu, K., Wu, Q., Su, R., Zhu, J., Yang, C., Dai, C., Liu, H.:

943   Improved Jayaweera-Mikkelsen model to quantify ammonia volatilization from rice paddy fields in

944   China, Environ. Sci. Pollut. R., 26, 8136-8147, doi:10.1007/s11356-019-04275-2, 2019.

945   Zhang, S., Cai, G., Wang, X., Xu, Y., Zhu, Z., Freney, J. R.: Losses of urea-nitrogen applied to maize

946   grown on a calcareous Fluvo-Aquic soil in North China Plain, Pedosphere, 171–178,

947   doi:10.1109/34.142909, 1992.

948   Zhang, W., Li, S., Han, S., Xie, H., Lu, C., Sui, Y., Rui, W., Liu, C., Yao, Z., Zheng, X.: Less intensive

949   nitrate leaching from Phaeozems cultivated with maize generally occurs in northeastern China, Agr.

950   Ecosyst. Environ., doi:10.1016/j.agee.2021.107303, 2021.

951   Zhang, W., Li, Y., Zhu, B., Zheng, X., Liu, C., Tang, J., Su, F., Zhang, C., Ju, X., Deng, J.: A

952   process-oriented hydro-biogeochemical model enabling simulation of gaseous carbon and nitrogen

953   emissions and hydrologic nitrogen losses from a subtropical catchment, Sci. Total Environ., 616,

954   305–317, doi:10.1016/j.scitotenv.2017.09.261, 2018.

955   Zhang, W., Yao, Z., Zheng, X., Liu, C., Rui, W., Wang, K., Li, S., Han, S., Zuo, Q., Shi, J.: Effects of

956   fertilization and stand age on N_2O and NO emissions from tea plantations: a site-scale study in a

957   subtropical region using a modified biogeochemical model, Atmos. Chem. Phys., 20, 6903–6919,

958   doi:10.5194/acp-20-6903-2020, 2020.

959   Zhao, X., Xie, Y., Xiong, Z., Yan, X., Xing, G., Zhu, Z.: Nitrogen fate and environmental consequence

960   in paddy soil under rice-wheat rotation in the taihu lake region, China, Plant Soil, 319, 225–234, doi:

961 10.1007/s11104-008-9865-0, 2009.

962 Zhou, F., Ciais, P., Hayashi, K., Galloway, J., Kim, D. G., Yang, C., Li, S., Liu, B., Shang, Z., Gao, S.:

963 Re-estimating NH_3 emissions from Chinese cropland by a new nonlinear model, Environ. Sci. Technol.,

964 50, 564–572, doi:10.1021/acs.est.5b03156, 2016.

965 Zhu, Z., Cai, G., Simpson, J. R., Zhang, S., Chen, D., Jackson, A. V., Freney, J. R.: Processes of nitrogen

966 loss from fertilizers applied to flooded rice fields on a calcareous soil in north–central China, Nutr. Cycl.

967 Agroecosys., 18, 101–115, doi:10.1007/BF01049507, 1989.

968 _______________________

969

LC
(37.8°N, 114.7°E)

QZ
(36.8°N, 115.0°E)

YJ
(34.9°N, 110.7°E)

DY
(32.0°N, 119.6°E)

YT
(31.3°N, 105.5°E)

YTA
(28.0°N, 117.0°E)

SZ
(22.6°N, 114.0°E)

DBW
(39.5°N, 116.3°E)

GC
(37.5°N, 115.9°E)

FQ
(35.0°N, 114.1°E)

CS
(31.5°N, 120.8°E)

● Upland
● Paddy
● Upland & Paddy

970
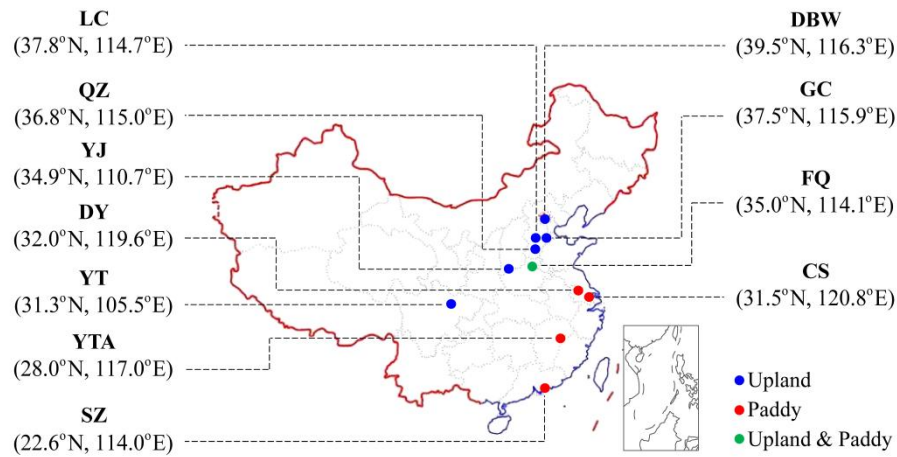
Fig. 1 Location of the experimental field sites involved in this study. The sites are Changshu (CS), Danyang (DY), Dongbeiwang (DBW), Fengqiu (FQ), Guangchuan (GC), Luancheng (LC), Quzhou (QZ), Shenzhen (SZ), Yanting (YT), Yingtan (YTA), and Yongji (YJ).

974

975
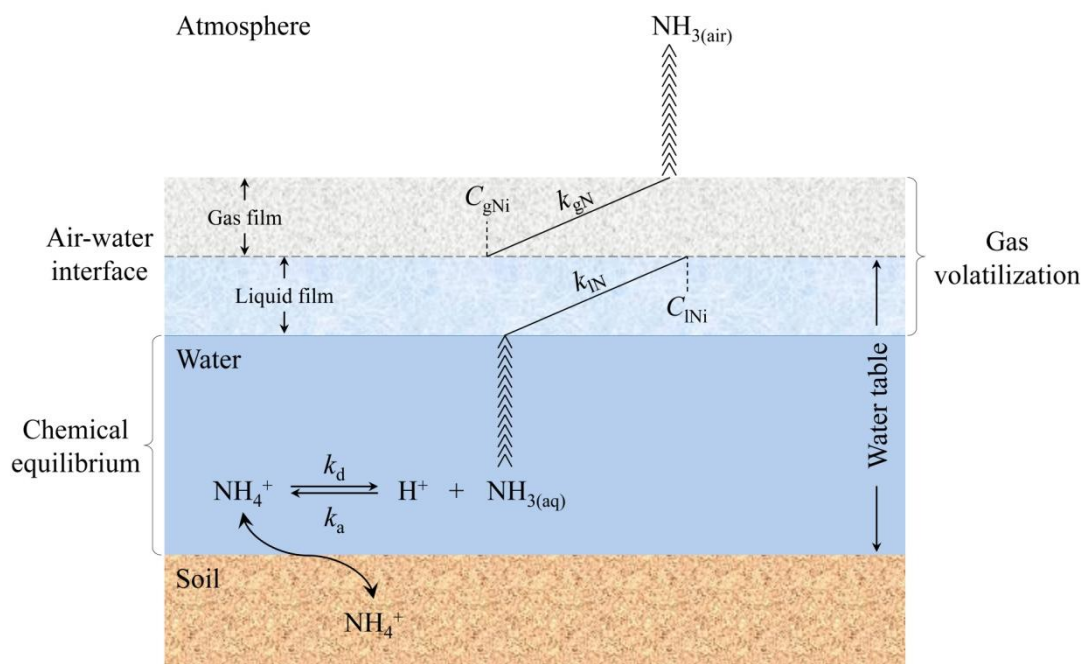
Fig. 2 Mechanism of the Jayaweera-Mikkelsen model introduced into the modified CNMM-DNDC.
k_d **and** k_a **are referred to as the dissociation and association rate constants for** NH_4^+/NH_3 **chemical**
equilibrium, respectively. k_{IN} **and** k_{gN} **are referred to as the exchange constants for** NH_3 **in the**
liquid and gas films, respectively. C_{INi} **and** C_{gNi} **are referred to as the average concentrations of** NH_3
at the interface in the liquid and gas films, respectively. $NH_{3(aq)}$ **and** $NH_{3(air)}$ **are referred to as the**
average concentration of NH_3 **in aqueous and gas phases, respectively.**

982

983
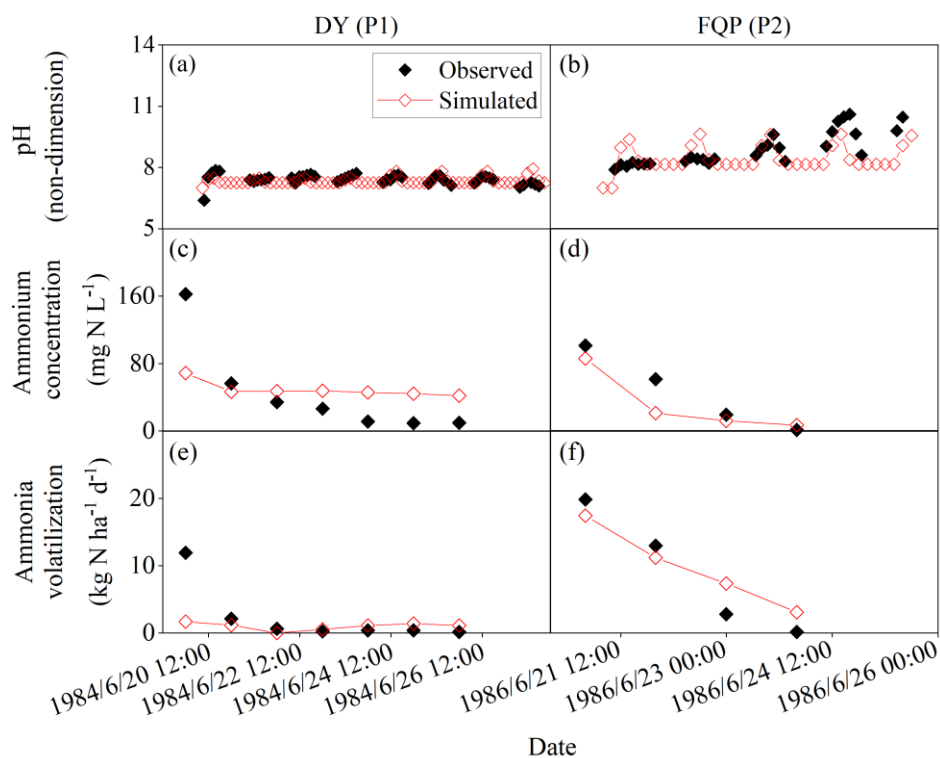
984 **Fig. 3 Observed and simulated pH and ammonium concentrations of floodwater and daily**

985 **ammonia volatilization from the ammonium carbonate application for DY and FQP. The**

986 **definitions of the case codes are referred to Table 2. The sites are Danyang (DY) and Fengqiu with**

987 **rice paddy fields (FQP).**

988

989
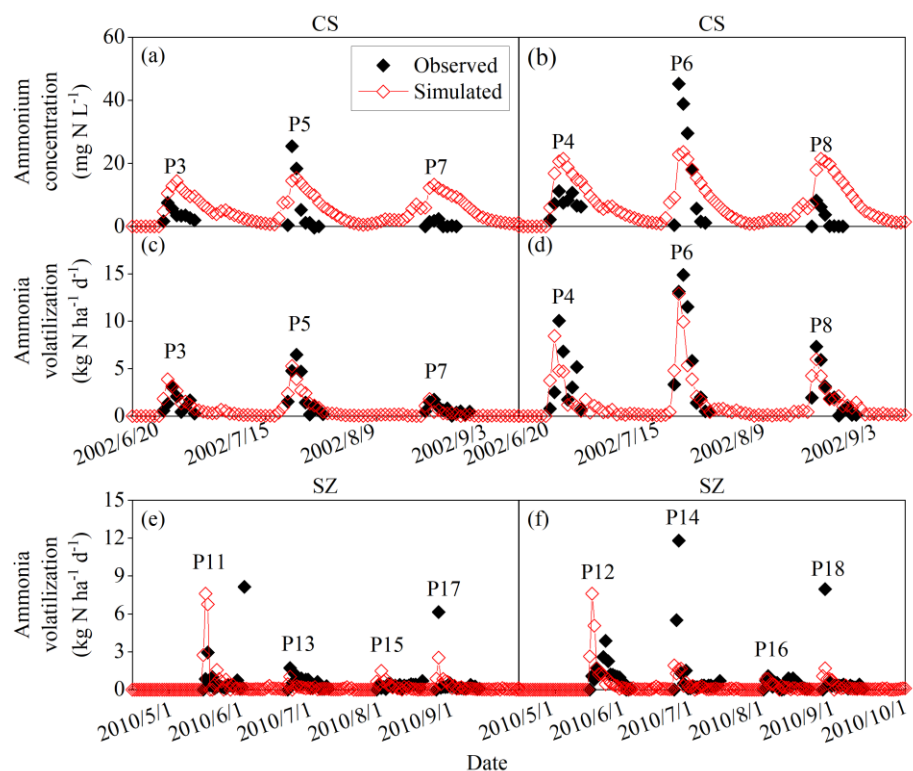
990 **Fig. 4 Observed and simulated ammonium concentrations of floodwater and daily ammonia**

991 **volatilization from the urea application for CS and SZ. The definitions of the case codes are**

992 **referred to Table 2. The sites are Changshu (CS) and Shenzhen (SZ).**

993

994
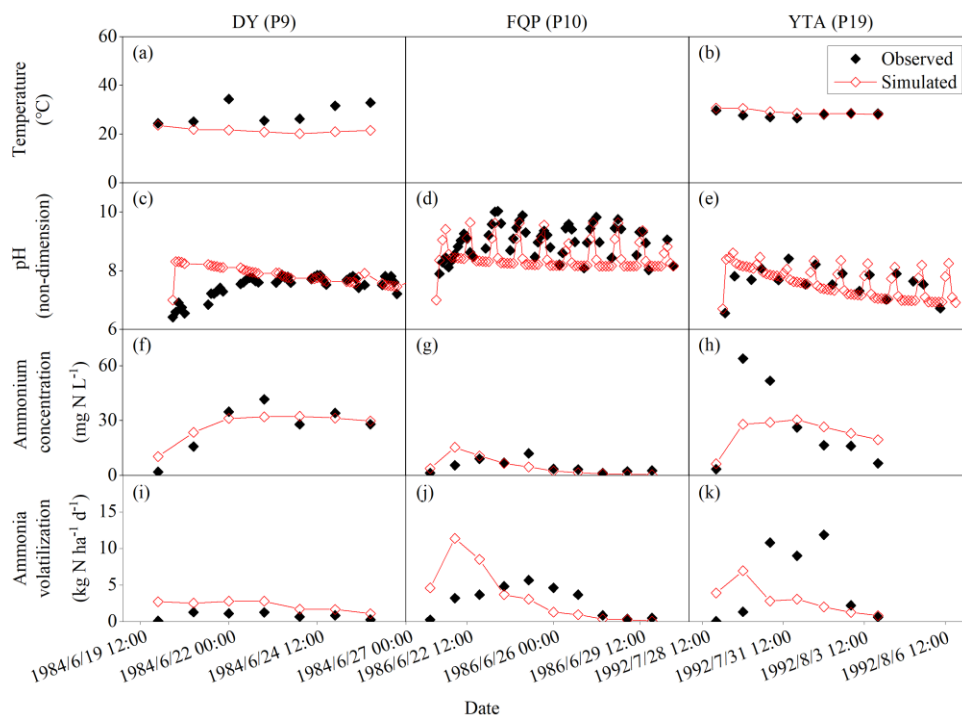
995 **Fig. 5 Observed and simulated temperatures, pH and ammonium concentrations of floodwater**
996 **and daily ammonia volatilization from the urea application for DY, FQP and YTA. The definitions**
997 **of the case codes are referred to Table 2. The sites are Danyang (DY), Fengqiu with rice paddy**
998 **fields (FQP) and Yingtan (YTA).**

999

1000

1001
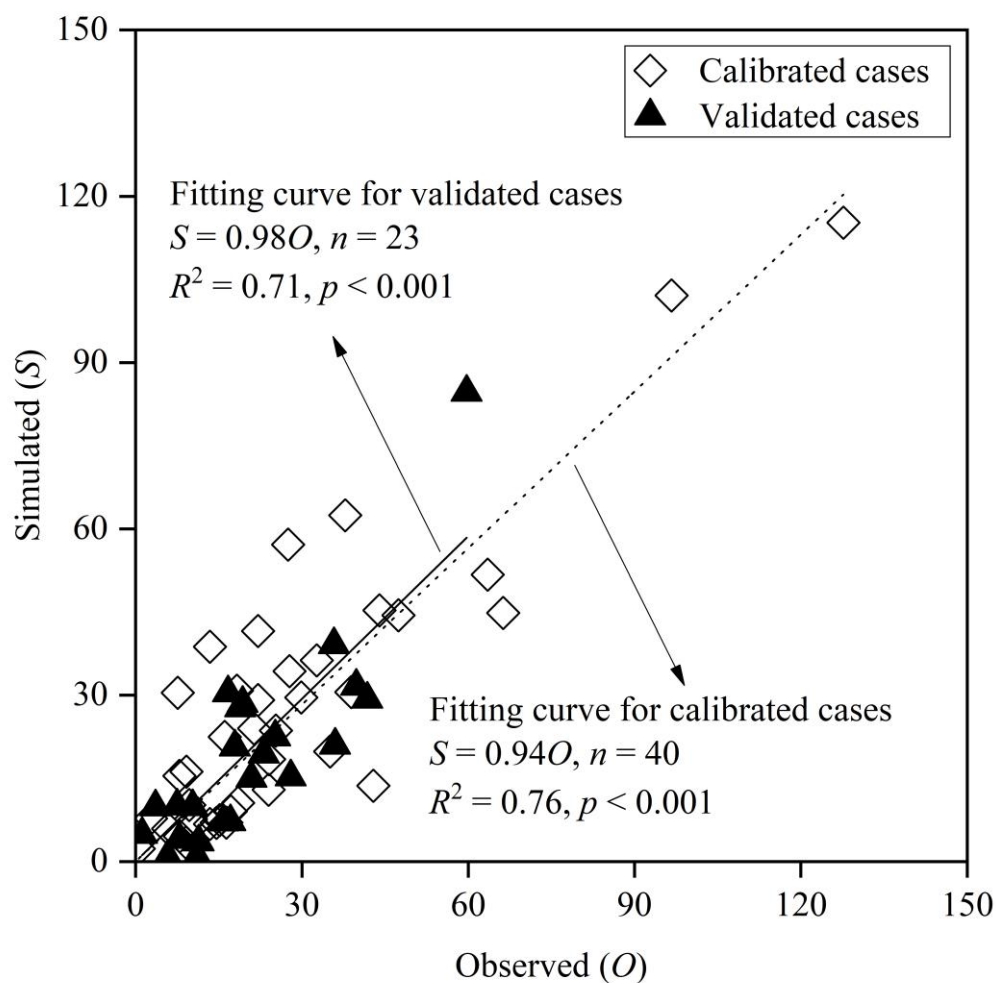
Fig. 6 Comparison between the observed and simulated cumulative ammonia volatilization across all calibrated and validated cases of upland and rice paddy fields. n, p and R^2 denote the sample size, significance level and coefficient of determination for the zero-intercept linear regression, respectively.

1006
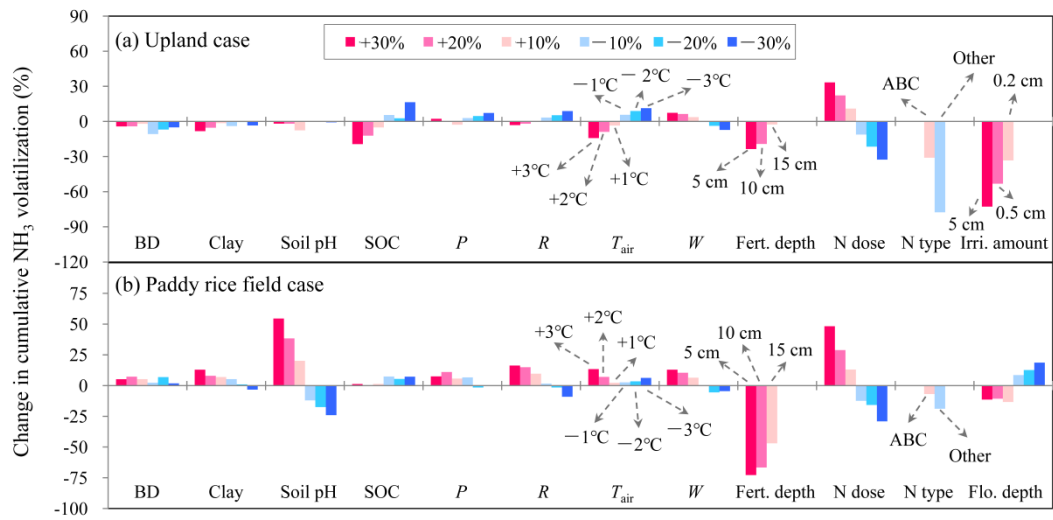
Fig. 7 Sensitivity analysis of the modified CNMM-DNDC in simulating cumulative ammonia (NH$_3$) volatilization from uplands and rice paddy fields during the measurement periods through change input factors. The investigated input factors include: 3-hourly averages of air temperature (T_{air}) and wind speed (W); 3-hourly totals of precipitation (P) and solar radiation (R) during individual measurement periods of NH$_3$ volatilization; soil clay fraction, pH, organic carbon (SOC) content and bulk density (BD); irrigation water amount (Irri. amount) and floodwater depth (Flo. depth); and, nitrogen fertilization depth, dose and type (Fert. depth, N dose, and N type, respectively). The N types include ammonium bicarbonate (ABC) and other ammonium-based nitrogen fertilizers (Other). The legends within the frame apply to all the subfigures and all the factors without notes highlighted by arrows.

1019
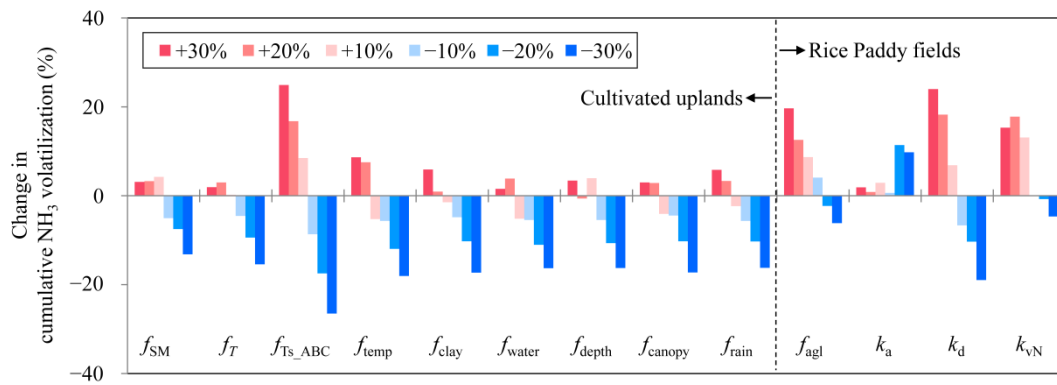
Fig. 8 Sensitivity analysis on the improved parameters of the modified CNMM-DNDC model in
simulating cumulative ammonia (NH$_3$) volatilization from cultivated uplands and rice paddy fields.
The improved parameters for simulating NH$_3$ volatilization from cultivated uplands involved in
the sensitivity analysis include: effect of soil moisture and soil temperature on urea hydrolysis (f_{SM}
and f_T), effect of soil temperature on ammonium bicarbonate decomposition (f_{Ts_ABC}), effect of soil
temperature, soil clay content, soil moisture, soil depth, dry canopy, rain wetting canopy on NH$_3$
volatilization (f_{temp}, f_{clay}, f_{water}, f_{depth}, f_{canopy} and f_{rain}). The improved parameters for simulating NH$_3$
volatilization from rice paddy fields involved in the sensitivity analysis include: the effect of algal
growth on floodwater pH (f_{alg}), the dissociation and association rate constants for NH$_4^+$/NH$_{3(aq)}$
equilibrium (k_d and k_a), and the volatilization rate constant of NH$_{3(aq)}$ (k_{vN}).

1031 **Table 1** Descriptive information of the studied experimental sites of rice paddy fields for model
1032 evaluation, including site name, experimental year (Year), crop rotation (Crop), fertilizer type (Type)
1033 and dose (Dose, kg N ha^{-1}), measurement method for ammonia volatilization (Method), number of
1034 fertilization cases (Number) and reference (Ref.).

Site [a]	Year	Crop [b]	Type	Dose	Method [d]	Number	Ref. [e]
CS	2002–2003	RW	Urea	41–135	MM	6	[1]
DY	1984	RW	Urea/ABC [c]	90	MM	2	[2]
FQP	1986	RW	Urea/ABC	90	MM	2	[3]
SZ	2010	DR	Urea	41–162	WT	8	[4]
YTA	1992	DR	Urea	90	MM	1	[5]

1035 [a] The sites are Changshu (CS), Danyang (DY), Fengqiu with rice paddy fields (FQP), Shenzhen (SZ),
1036 and Yingtan (YTA).
1037 [b] The presented crop rotation types are rice–wheat (RW) and double rice (DR).
1038 [c] ABC is the abbreviation of ammonium bicarbonate.
1039 [d] The presented methods for the measurement of ammonia volatilization are wind tunnel (WT) and
1040 micrometeorological technique (MM).
1041 [e] [1] Song et al., 2004; [2] Cai et al., 1986; [3] Zhu et al., 1989; [4] Gong et al., 2013; and [5] Cai et al.,
1042 1992.

Table 2 Observed and simulated cumulative ammonia volatilization during the measurement periods, model biases, and management practices of individual fertilizer application cases in the rice paddy fields.

Case code [a]	Site [b]	Period	O [c]	S [c]	RMB [c]	Water table [d]	Pre [e]	Fertilizer application Type [f]	Method [g]	Dose [h]
P1 [@]	DY	Jun. 20 to Jun. 26, 1984	16.4	7.04	−57.0	5	0	ABC	BFT5	90
P2	FQP	Jun. 21 to Jun. 30, 1986	35.8	39.13	9.3	4	0.18	ABC	BFT5	90
P3	CS	Jun. 22 to Jun. 30, 2002	10.3	9.89	−4.0	4 [*]	6.38	Urea	B	40.5
P4	CS	Jun. 22 to Jun. 30, 2002	23.1	19.40	−16.0	4 [*]	6.38	Urea	B	81
P5	CS	Jul. 20 to Jul. 29, 2002	20.9	15.04	−28.0	4 [*]	0.54	Urea	B	54
P6	CS	Jul. 20 to Jul. 29, 2002	39.8	31.61	−20.6	4 [*]	0.54	Urea	B	108
P7	CS	Aug. 20 to Aug. 31, 2002	7.5	10.02	33.6	4 [*]	3.07	Urea	B	40.5
P8	CS	Aug. 20 to Aug. 31, 2002	17.9	20.68	15.5	4 [*]	3.07	Urea	B	81
P9 [@]	DY	Jun. 20 to Jun. 26, 1984	7.9	15.44	94.9	5	0	Urea	BFT5	90
P10 [@]	FQP	Jun. 21 to Jun. 30, 1986	27.8	34.32	23.7	4	0.18	Urea	BFT5	90
P11 [@]	SZ	May 16 to Jun. 4, 2010	16.1	22.50	39.8	7.5 [#]	0	Urea	B	162.2
P12 [@]	SZ	May 16 to Jun. 4, 2010	21.4	24.00	12.2	7.5 [#]	0	Urea	B	162.2
P13 [@]	SZ	Jun. 22 to Jul. 11, 2010	9.1	3.43	−62.4	7.5 [#]	0	Urea	B	40.9
P14 [@]	SZ	Jun. 22 to Jul. 11, 2010	17.2	9.07	−47.3	7.5 [#]	0	Urea	B	81.8
P15 [@]	SZ	Jul. 31 to Aug. 19, 2010	5.9	5.92	0.3	7.5 [#]	0	Urea	B	40.9
P16 [@]	SZ	Jul. 31 to Aug. 19, 2010	8.0	4.57	−42.9	7.5 [#]	0	Urea	B	40.9
P17 [@]	SZ	Aug. 26 to Sep. 14, 2010	10.0	7.66	−23.4	7.5 [#]	0	Urea	B	81.8
P18 [@]	SZ	Aug. 26 to Sep. 14, 2010	13.4	6.79	−49.3	7.5 [#]	0	Urea	B	81.8
P19	YTA	Jul. 29 to Aug. 6, 1992	36.0	20.98	−41.7	2	1.36	Urea	BFT5	90

[a] P1 to P19 encode the experimental cases following individual application events of synthetic nitrogen fertilizers; the superscript "@" symbol marks the cases with the ammonia observations being referred to the model calibration.

[b] The sites are Changshu (CS), Danyang (DY), Fengqiu with rice paddy fields (FQP), Shenzhen (SZ), and Yingtan (YTA).

[c] O and S are the cumulative NH_3 volatilization (kg N ha^{-1}) observed and simulated by the modified CNMM-DNDC, respectively; RMB is the relative model bias (%) of the modified model, each of which was determined as the relative difference between the simulated and observed values.

[d] The depth of floodwater table (cm). For the cases with "*" and "#", the exact depth of the floodwater table was not reported. The floodwater table depth of the cases with "*" was arbitrarily set as the traditional depth of the floodwater table of the DY site, which was located in the same region. The floodwater depths of the cases with "#" were set by model calibration.

[e] Pre denotes total rainfall (cm) during the experimental period(s).

[f] ABC is the fertilizer type of ammonium bicarbonate.

[g] The application methods are surface broadcast (B) and broadcast followed by tillage (BFT). The figures following BFT are the depth in soil (cm).

[h] Unit: kg N ha^{-1}.

Table 3 Statistical indices for evaluating the performance of the modified CNMM-DNDC in simulating daily and cumulative ammonia (NH_3) fluxes from ammonium bicarbonate (ABC) and urea (including other fertilizer types) applications for the independent calibration (Cal) and validation (Val) cases in uplands and rice paddy fields.

Land use	NH_3 flux	Fertilizer type	Operation	Num	IA	NSI	ZIR Slope	R^2	p
Upland	Daily	ABC	Cal	39	0.5	−1.34	0.53	na	na
			Val	24	0.60	−0.51	0.69	na	na
		Urea	Cal	287	0.44	−0.06	0.38	na	na
			Val	137	0.67	0.02	0.64	0.09	< 0.001
	Cumulative	ABC	Cal	3	0.75	0.14	0.73	0.64	ns
			Val	2	–	–	–	–	–
		Urea	Cal	26	0.93	0.73	0.94	0.71	< 0.001
			Val	13	0.91	0.49	1.06	0.74	< 0.001
Rice paddy field	Daily	ABC	Cal	7	0.33	0.02	0.16	na	na
			Val	4	0.94	0.85	0.90	0.71	ns
		Urea	Cal	176	0.53	−0.35	0.47	0.04	< 0.05
			Val	63	0.72	0.36	0.56	0.19	< 0.001
	Cumulative	ABC	Cal	1	–	–	–	–	–
			Val	1	–	–	–	–	–
		Urea	Cal	10	0.88	0.30	1.03	0.68	< 0.01
			Val	7	0.85	0.60	0.77	0.65	< 0.05

The statistical indices are the index of agreement (IA), Nash–Sutcliffe Index (NSI), and the slope, determination coefficient (R^2) and significance level (p) of the zero-intercept univariate linear regression (ZIR) of observations against simulations. Being not available (na) indicates a negative R^2 and a suffering F-test. Being not significant (ns) indicates a ZIR with $p > 0.05$. Num is the abbreviation of sample number.

Table 4 Statistical indices for evaluating the performance of the CNMM-DNDC in simulating the daily temperature (T), pH and ammonium concentration (NH_4^+) in floodwater for the calibration (Cal) and validation (Val) cases.

Variables	Operation	Num	Cases	IA	NSI	ZIR		
						Slope	R^2	p
T	Cal	7	P9	0.43	–3.50	1.32	na	na
	Val	7	P19	0.51	–1.76	0.96	na	na
pH	Cal	147	P1, P9, P10	0.83	0.55	1.00	0.55	< 0.001
	Val	45	P2, P19	0.79	0.36	1.01	0.36	< 0.001
NH_4^+	Cal	24	P1, P9, P10	0.78	0.48	1.03	0.48	< 0.001
	Val	55	P2, P3–P8	0.68	0.25	0.74	0.34	< 0.001

1075   The statistical indices are the index of agreement (IA), Nash–Sutcliffe Index (NSI), and the slope, determination coefficient (R^2) and significance level (p) of the zero-intercept univariate linear regression (ZIR) of observations against simulations. Being not available (na) indicates a negative R^2 and a suffering F-test. Being not significant (ns) indicates a ZIR with $p > 0.05$. Num is the abbreviation of sample number. The definitions of the case codes are referred to Table 2.